TABLE I. Genotype Nature of the Eleven Gene Segments of Group A Rotavirus (GAR) Strain B12 Sequenced in This Study With Those of Selected Human and Animal GAR Strains With Known Genomic Constellations

	Genotypes										
Strain/host	VP7	VP4	VP6	VP1	VP2	VP3	NSP1	NSP2	NSP3	NSP4	NSP5
B12/Hu	G8	P[1]	I2	R2	C2	M2	A3	N2	T6	E2	H3
NIC522[a]/Hu	G8	P[1]	I2	R2	C2	M2	A13	N2	T2	E2	H3
HMG035/Hu	G8	P[1]					A11				
MP409/Hu	G8	P[1]					A11		T6	E2	
O/Bo	G8	P[1]					A11	N2			
A5/Bo	G8	P[1]					A14				
Arg/Rio Negro/98/Gu	G8	P[1]	I2	R5	C2	M2	A11	N2	T6	E12	H3
GER1H-09/Hu	G8	P[4]	I2	R2	C2	M2	A2	N2	T2	E2	H2
DRC86/ Hu	G8	P[6]	I2	R2	C2	M2	A2	N2	T2	E2	H2
DRC88/ Hu	G8	P[8]	I2	R2	C2	M2	A2	N2	T2	E2	H2
69M/Hu	G8	P[10]	I2	R2	C2	M2	A2	N2	T2	E2	H2
Sun9/Bo	G8	P[14]	I2	R2	C2	M2					
OVR762/Ov	G8	P[14]	I2	R2	C2	M2	A11	N2	T6	E2	H3
Arg/chubut/99/Gu	G8	P[14]	I2	R5	C2	M2	A3	N2	T6	E12	H3
BP1062/04/Hu	G8	P[14]	I2	R2	C2	M2	A11	N2	T6	E2	H3
B1711/Hu	G6	P[6]	I2	R2	C2	M2	A2	N2	T2	E2	H2
PA169/Hu	G6	P[14]	I2	R2	C2	M2	A3	N2	T6	E2	H3
Hun5/Hu	G6	P[14]	I2	R2	C2	M2	A11	N2	T6	E2	H3
111/05-27/Hu	G6	P[14]	I2	R2	C2	M2	A3	N2	T6	E2	H3
MG6/Hu	G6	P[14]	I2	R2	C2	M2	A11	N2	T6	E2	H3
B10925-97/Hu	G6	P[14]	I2	R2	C2	M2	A3	N2	T6	E2	H3
BP1879/03/Hu	G6	P[14]	I2	R2	C2	M2	A11	N2	T6	E2	H3
NCDV/Bo	G6	P[1]	I2	R2	C2	M2	A3	N2	T6	E2	H3
WC3/Bo	G6	P[5]	I2	R2	C2	M2	A3	N2	T6	E2	H3
UK/Bo	G6	P[5]	I2	R2	C2	M2	A3	N2	T7	E2	H3
RC-18/08/An	G6	P[14]	I2	R2	C2	M2	A11	N2	T6	E2	H3
GO34/Cap	G6	P[1]	I2	R2	C2	M2	A11	N2	T6	E2	H3
A64/Hu	G10	P[14]	I2	R2	C2	M1	A3	N2	T6	E2	H3

An, antelope; Bo, bovine; Cap, caprine; Gu, guanaco; Hu, human; Ov, ovine.
Dark gray indicates the gene segments with a genotype identical to that of strain B12, while lighter shade of gray indicates the genome segments with a different genotype.
[a]Genotype assignment based on partial-length nucleotide sequences [Banyai et al., 2009]. To our knowledge, to date, the nucleotide sequence accession numbers for the partial-length gene sequences of strain NIC522 are not available in the GenBank database.

OVR762 (Fig. 1J). The NSP5 gene of strain B12 exhibited high nucleotide sequence identities of 97.0–97.5% and 96.9% to those of human G6P[14] and ruminant strains, respectively (Table II), and by phylogenetic analysis, clustered with human G6P[14] strains 111/05-27 and PA169 and ovine strain OVR762 (Fig. 1K).

Taken together, each of the 11 genes of strain B12 appeared to be more related to cognate genes of artiodactyl (ruminant and/or camelid) and/or artiodactyl-derived human strains than those of most other rotaviruses. Strain B12 exhibited low levels of genetic relatedness to canonical human GAR strains, such as Wa and DS-1. Although 6 out of the 11 genes of strain B12 belonged to the same genotype as strain DS-1, within these genotypes, strain B12 exhibited low nucleotide sequence identities to and clustered separately from strain DS-1 (Fig. 1A–K, Table II). These observations excluded the possibility that strain B12 might have originated from reassortment events between artiodactyl-like human and true human GAR strains. Therefore, G8P[1] strain B12 might have been directly transmitted from artiodactyls to humans. Unhygienic conditions and close proximity of humans to livestock at the sampling site might have facilitated such an event. Unfortunately, none of the animals from the sampling site were screened for the presence of rotaviruses. Similar to the artiodactyl-like human P[14] strains reported so far [Matthijnssens et al., 2009; Banyai et al., 2010], strain B12 did not exhibit similar levels of relatedness for all the 11 gene segments, suggesting possible reassortment event(s) that might have occurred among strains of different artiodactyl host species preceding transmission to humans. This hypothesis on the independent zoonotic origin of B12 was corroborated by (i) few reports on detection of G8P[1] strains in humans and from distant geographical locations; (ii) differences in the origin of the available gene sequences of G8P[1] strains HMG035 and MP409 with those of B12, although it remains to be determined whether strains HMG035 and MP409 originated from animal–human reassortment events or are zoonotic strains; and (iii) lack of evidence for efficient human-to-human transmission of G8P[1] or other artiodactyl-like human strains, though few such strains have been reported to date. Several artiodactyl host species (buffaloes, bushbucks, camels, cattle, gazelles, giraffes, goats, impalas, reedbucks, rhinos, sheep, waterbucks, and zebras) are found in the Nakuru district of Kenya.

Although strain NIC522, the only confirmed zoonotic G8P[1] strain to date, was associated with diarrhea,

TABLE II. Nucleotide Sequence Identities (%) of the 11 Gene Segments of Group A Rotavirus (GAR) Strain B12 to Those of Selected Human and Animal GAR Strains

	Nucleotide sequence identities (%)										
Strain/host/G-P combination	VP7	VP4	VP6	VP1	VP2	VP3	NSP1	NSP2	NSP3	NSP4	NSP5
HMG035/Hu/G8P[1]	84.8	80.7	—	—	—	—	65.9	—	—	—	—
MP409/Hu/G8P[1]	83.2	80.3	—	—	—	—	73.7	—	91.0	87.2	—
GER1H-09/Hu/G8P[4]	84.2	70.2	93.0	85.7	85.2	83.7	67.1	91.4	78.6	92.3	71.7
DRC86/ Hu/G8P[6]	84.7	70.8	93.1	85.9	85.9	83.8	67.5	87.3	79.5	91.2	71.4
DRC88/ Hu/G8P[8]	84.6	69.7	93.1	85.9	85.6	83.8	67.7	87.3	79.4	90.9	71.2
69M/Hu/G8P[10]	88.6	73.9	93.7	85.3	88.6	88.7	67.5	95.6	77.9	94.1	85.8
BP1062/04/Hu/G8P[14]	84.7	68.9	94.2	85.8	86.8	83.5	75.4	87.7	91.5	93.9	94.8
B1711/Hu/G6P[6]	75.7	70.9	92.8	85.2	85.8	88.7	67.5	87.7	78.9	90.3	85.3
PA169/Hu/G6P[14]	75.7	68.2	96.3	91.3	85.9	88.8	93.6	92.7	95.3	92.7	97.0
Hun5/Hu/G6P[14]	76.2	69.1	88.3	85.4	89.4	83.7	76.0	92.4	92.2	93.2	95.2
111/05-27/Hu/G6P[14]	75.6	69.0	95.6	85.5	88.0	84.4	93.0	96.8	90.5	92.8	97.0
MG6/Hu/G6P[14]	75.9	68.8	93.0	93.9	88.9	82.6	75.0	89.1	94.0	94.4	96.4
B10925-97/Hu/G6P[14]	76.3	69.1	94.3	85.7	88.2	83.7	92.9	92.5	90.9	92.9	97.5
BP1879/03/Hu/G6P[14]	77.0	68.7	94.2	85.6	88.1	85.4	75.0	92.4	92.0	93.9	95.5
A64/Hu//G10P[14]	74.5	67.7	94.2	85.3	88.3	75.8	97.6	97.6	92.6	94.9	91.5
NCDV/Bo/G6P[1]	75.7	79.8	96.8	94.9	90.0	88.5	98.4	89.6	95.2	90.0	96.9
WC3/Bo/G6P[5]	76.0	69.1	95.8	95.1	89.4	87.8	97.0	89.7	95.3	84.6	96.9
UK/Bo/G6P[5]	76.6	69.3	96.1	92.2	88.5	88.2	89.0	88.9	83.4	92.1	93.1
O/Bo/G8P[1]	96.3	79.6	—	—	—	—	74.4	88.7	—	—	—
A5/Bo/G8P[1]	84.0	80.8	—	—	—	—	75.3	—	—	—	—
Sun9/Bo/G8P[14]	94.1	67.5	95.5	94.5	88.8	88.0	—	—	—	—	—
RC-18/08/An/G6P[14]	75.5	68.5	94.8	95.6	89.1	89.2	74.7	94.2	89.6	91.5	95.7
GO34/Cap/G6P[1]	76.5	80.7	92.3	85.6	87.3	83.2	73.9	88.9	92.4	92.0	94.3
Arg/chubut/99/Gu/G8P[14]	97.2	68.6	93.0	81.4	88.5	87.2	86.0	88.7	98.0	88.1	95.7
Arg/Rio Negro/98/Gu/G8P[1]	97.0	81.8	93.1	81.3	88.6	88.1	74.7	86.9	89.5	88.5	93.0
OVR762/Ov/G8P[14]	95.1	67.7	94.1	86.1	88.2	83.6	74.2	91.8	91.0	92.7	96.9
DS-1/Hu/G2P[4]	72.4	69.8	86.5	85.7	85.7	84.1	66.9	87.6	78.6	89.4	85.2
Wa/Hu/G1P[8]	72.7	70.2	79.7	78.9	80.2	76.0	66.6	84.1	83.0	83.1	86.1

An, antelope; Bo, bovine; Cap, caprine; Gu, guanaco; Hu, human; Ov, ovine.
Shade of gray indicates the maximum nucleotide sequence identity exhibited by strain B12 for each of the 11 gene segments. "—" indicates that no sequence data were available in the GenBank database.

another human strain was also detected in the same stool sample, as revealed by detection of a human rotavirus genotype I1 VP6 gene [Banyai et al., 2009], raising doubts on the role of NIC522 in causing diarrhea. The other two G8P[1] strains, HMG035 and MP409, were also detected from diarrheal stool samples; however, whether these strains were transmitted directly from artiodactyls to humans or are animal–human reassortants remain to be ascertained, although by hybridization studies, HMG035 was closely related to a local bovine strain [Jagannath et al., 2000; Adah et al., 2001, 2003]. On the other hand, strain B12 was detected from an asymptomatic infant. It might be possible that B12, being of animal origin, failed to cause diarrhea in humans, as was reported previously for other animal-derived rotavirus G9P[11] and G10P[11] strains [Rao et al., 2003]. However, a subsequent study had reported G10P[11] strains, similar genetically to the asymptomatic strains, in diarrheal stools of children [Ramani et al., 2009]. The other possibility may be maternal immunity conferred by breast feeding, a practice common in this area. Zoonotic rotavirus strains, although reported rarely, have been associated with diarrhea in humans [Varghese et al., 2004, 2006; Matthijnssens et al., 2006a, 2009; Tsugawa and Hoshino, 2008; Martella et al., 2009; Banyai et al., 2010], and therefore, information on additional zoonotic G8P[1] strains are required to ascertain the role of these viruses in human diarrhea.

Annually, rotavirus infection causes 4,471 deaths, 8,781 hospitalizations, and 1,443,883 clinic visits in Kenya [Tate et al., 2009]. However, to date, only the VP7 and/or VP4 genes of a few Kenyan strains have been analyzed by RT-PCR-based genotyping and/or nucleotide sequencing [Kiulia et al., 2008, 2009; Esona et al., 2010; Nokes et al., 2010; Nyangao et al., 2010]. These limited studies revealed an increase in the detection of human G8 and G9 strains [Kiulia et al., 2008, 2009; Nokes et al., 2010; Nyangao et al., 2010]. To date, G8 strains in conjunction with P[4], P[6], P[8], P[11], or unknown P genotypes have been reported from Kenya [Nakata et al., 1999; Cunliffe et al., 2001; Kiulia et al., 2008, 2009; Esona et al., 2010; Nokes et al., 2010; Nyangao et al., 2010]. In African nations such as Kenya, the presence of poor hygienic conditions and close contact between humans and animals offer an ideal environment for complex animal–human reassortment and/or interspecies transmission events, as evidenced by full genomic analyses of B12 and other African G8 strains [Matthijnssens et al., 2006b; Esona et al., 2009]. Therefore, determination of full genome sequences of the other Kenyan G8 and unconventional strains might be of great significance in context to studies on zoonosis and

genetic diversity of rotaviruses. To our knowledge, GAR G8P[1] strain B12 is the first report on the full genome of a Kenyan rotavirus strain, and might be the oldest G8 strain molecularly characterized from the African continent. Strain B12 also represented a rare instance of animal-to-human interspecies transmission of rotaviruses.

REFERENCES

Adah MI, Nagashima S, Wakuda M, Taniguchi K. 2003. Close relationship between G8-serotype bovine and human rotaviruses isolated in Nigeria. J Clin Microbiol 41:3945–3950.

Adah MI, Wade A, Taniguchi K. 2001. Molecular epidemiology of rotaviruses in Nigeria: Detection of unusual strains with G2P[6] and G8P[1] specificities. J Clin Microbiol 39:3969–3975.

Adah MI, Rohwedder A, Olaleyle OD, Werchau H. 1997. Nigerian rotavirus serotype G8 could not be typed by PCR due to nucleotide mutation at the 3' end of the primer binding site. Arch Virol 142:1881–1887.

Banyai K, Esona MD, Mijatovic S, Kerin TK, Pedreira C, Mercado J, Balmaseda A, Perez MC, Patel MM, Gentsch JR. 2009. Zoonotic bovine rotavirus strain in a diarrheic child, Nicaragua. J Clin Virol 46:391–393.

Banyai K, Papp H, Dandar E, Molnar P, Mihaly I, Van Ranst M, Martella V, Matthijnssens J. 2010. Whole genome sequencing and phylogenetic analysis of a zoonotic human G8P[14] rotavirus strain. Infect Genet Evol 10:1140–1144.

Cashman O, Lennon G, Sleator RD, Power E, Fanning S, O'Shea H. 2010. Changing profile of the bovine rotavirus G6 population in the south of Ireland from 2002 to 2009. Vet Microbiol DOI: 10.1016/j.vetmic.2010.05.012. (in press).

Chandrahasen C, Grimwood K, Redshaw N, Rich FJ, Wood C, Stanley J, Kirman JR. 2010. New Zealand Rotavirus Study Group. Geographical differences in the proportion of human group A rotavirus strains within New Zealand during one epidemic season. J Med Virol 82:897–902.

Cunliffe NA, Dove W, Bunn JE, Ben Ramadam M, Nyangao JW, Riveron RL, Cuevas LE, Hart CA. 2001. Expanding global distribution of rotavirus serotype. G9: Detection in Libya, Kenya, and Cuba. Emerg Infect Dis 7:890–892.

Esona MD, Geyer A, Page N, Trabelsi A, Fodha I, Aminu M, Agbaya VA, Tsion B, Kerin TK, Armah GE, Steele AD, Glass RI, Gentsch JR. 2009. Genomic characterization of human rotavirus G8 strains from the African rotavirus network: Relationship to animal rotaviruses. J Med Virol 81:937–951.

Esona MD, Steele D, Kerin T, Armah G, Peenze I, Geyer A, Page N, Nyangao J, Agbaya VA, Trabelsi A, Tsion B, Aminu M, Sebunya T, Dewar J, Glass R, Gentsch J. 2010. Determination of the G and P types of previously nontypeable rotavirus strains from the African rotavirus network, 1996–2004: Identification of unusual G types. J Infect Dis 202:S49–S54.

Estes MK, Kapikian AZ. 2007. Rotaviruses. In: Knipe DM, Howley PM, et al. editors. Fields virology, 5th edition. Philadelphia, PA: Lippincott Williams & Wilkins. pp 1917–1974.

Gentsch JR, Glass RI, Woods P, Gouvea V, Gorziglia M, Flores J, Das BK, Bhan MK. 1992. Identification of group A rotavirus gene 4 types by polymerase chain reaction. J Clin Microbiol 30:1365–1373.

Gentsch JR, Laird AR, Bielfelt B, Griffin DD, Banyai K, Ramachandran M, Jain V, Cunliffe NA, Nakagomi O, Kirkwood CD, Fischer TK, Parashar UD, Bresee JS, Jiang B, Glass RI. 2005. Serotype diversity and reassortment between human and animal rotavirus strains: Implications for rotavirus vaccine programs. J Infect Dis 192:S146–S159.

Gerna G, Sarasini A, Zentilin L, Di Matteo A, Miranda P, Parea M, Battaglia M, Milanesi G. 1990. Isolation in Europe of 69 M-like (serotype 8) human rotavirus strains with either subgroup I or II specificity and a long RNA electropherotype. Arch Virol 112:27–40.

Ghosh S, Alam MM, Ahmed MU, Talukdar RI, Paul SK, Kobayashi N. 2010a. The complete genome constellation of a caprine group A rotavirus strain reveals common evolution with ruminant and human rotavirus strains. J Gen Virol 91:2367–2373.

Ghosh S, Kobayashi N, Nagashima S, Chawla-Sarkar M, Krishnan T, Ganesh B, Naik TN. 2010b. Full genomic analysis and possible origin of a porcine G12 rotavirus strain RU172. Virus Genes 40:382–388.

Ghosh S, Varghese V, Samajdar S, Bhattacharya SK, Kobayashi N, Naik TN. 2006. Molecular characterization of a porcine Group A rotavirus strain with G12 genotype specificity. Arch Virol 151:1329–1344.

Greenberg HB, Estes MK. 2009. Rotaviruses: From pathogenesis to vaccination. Gastroenterology 136:1939–1951.

Hasegawa A, Inouye S, Matsuno S, Yamaoka K, Eko R, Suharyono W. 1984. Isolation of human rotaviruses with a distinct RNA electrophoretic pattern from Indonesia. Microbiol Immunol 28:719–722.

Heiman EM, McDonald SM, Barro M, Taraporewala ZF, Bar-Magen T, Patton JT. 2008. Group A human rotavirus genomics: Evidence that gene constellations are influenced by viral protein interactions. J Virol 82:11106–11116.

Herring AJ, Inglis NF, Ojeh CK, Snodgrass DR, Menzies JD. 1982. Rapid diagnosis of rotavirus infection by direct detection of viral nucleic-acid in silver-stained polyacrylamide gels. J Clin Microbiol 16:473–477.

Isegawa Y, Nakagomi O, Nakagomi T, Ishida S, Uesugi S, Ueda S. 1993. Determination of bovine rotavirus G and P serotypes by polymerase chain reaction. Mol Cell Probes 7:277–284.

Jagannath MR, Vethanayagam RR, Reddy BSY, Raman S, Rao CD. 2000. Characterization of human symptomatic rotavirus isolates MP409 and MP480 having 'long' RNA electropherotype and subgroup I specificity, highly related to the P6[1], G8 type bovine rotavirus A5, from Mysore, India. Arch Virol 145:1339–1357.

Kapikian AZ, Hoshino Y, Chanock RM. 2001. Rotaviruses. In: Knipe DM, Howley PM, et al. editors. Fields virology, 4th edition. Philadelphia, PA: Lippincott Williams and Wilkins. pp 1787–1883.

Kiulia NM, Kamenwa R, Irimu G, Nyangao JO, Gatheru Z, Nyachieo A, Steele AD, Mwenda JM. 2008. The epidemiology of human rotavirus associated with diarrhoea in Kenyan children: A review. J Trop Pediatr 54:401–405.

Kiulia NM, Nyaundi JK, Peenze I, Nyachieo A, Musoke RN, Steele AD, Mwenda JM. 2009. Rotavirus infections among HIV-infected children in Nairobi, Kenya. J Trop Pediatr 55:318–323.

Le VP, Kim JY, Cho SL, Nam SW, Lim I, Lee HJ, Kim K, Chung SI, Song W, Lee KM, Rhee MS, Lee JS, Kim W. 2008. Detection of unusual rotavirus genotypes G8P[8] and G12P[6] in South Korea. J Med Virol 80:175–182.

Martella V, Banyai K, Matthijnssens J, Buonavoglia C, Ciarlet M. 2009. Zoonotic aspects of rotaviruses. Vet Microbiol 140:246–255.

Matthijnssens J, Ciarlet M, Heiman E, Arijs I, Delbeke T, McDonald SM, Palombo EA, Iturriza-Gómara M, Maes P, Patton JT, Rahman M, Van Ranst M. 2008a. Full genome-based classification of rotaviruses reveals a common origin between human Wa-Like and porcine rotavirus strains and human DS-1-like and bovine rotavirus strains. J Virol 82:3204–3219.

Matthijnssens J, Ciarlet M, Rahman M, Attoui H, Banyai K, Estes MK, Gentsch JR, Iturriza-Gomara M, Kirkwood CD, Martella V, Mertens PP, Nakagomi O, Patton JT, Ruggeri FM, Saif LJ, Santos N, Steyer A, Taniguchi K, Desselberger U, Van Ranst M. 2008b. Recommendations for the classification of group A rotaviruses using all 11 genomic RNA segments. Arch Virol 153:1621–1629.

Matthijnssens J, Potgieter CA, Ciarlet M, Parreno V, Martella V, Banyai K, Garaicoechea L, Palombo EA, Novo L, Zeller M, Arista S, Gerna G, Rahman M, Van Ranst M. 2009. Are human P[14] rotavirus strains the result of interspecies transmissions from sheep or other ungulates that belong to the mammalian order Artiodactyla? J Virol 83:2917–2929.

Matthijnssens J, Rahman M, Martella V, Xuelei Y, De Vos S, De Leener K, Ciarlet M, Buonavoglia C, Van Ranst M. 2006a. Full genomic analysis of human rotavirus strain B4106 and lapine rotavirus strain 30/96 provides evidence for interspecies transmission. J Virol 80:3801–3810.

Matthijnssens J, Rahman M, Yang X, Delbeke T, Arijs I, Kabue JP, Muyembe JJ, Van Ranst M. 2006b. G8 rotavirus strains isolated in the Democratic Republic of Congo belong to the DS-1-like genogroup. J Clin Microbiol 44:1801–1809.

Nakata S, Gatheru Z, Ukae S, Adachi N, Kobayashi N, Honma S, Muli J, Ogaja P, Nyangao J, Kiplagat E, Tukei PM, Chiba S. 1999. Epidemiological study of the G serotype distribution of group A rotaviruses in Kenya from 1991 to 1994. J Med Virol 58:296–303.

Nokes DJ, Peenze I, Netshifhefhe L, Abwao J, De Beer MC, Seheri M, Williams TN, Page N, Steele D. 2010. Rotavirus genetic diversity,

disease association, and temporal change in hospitalized rural Kenyan children. J Infect Dis 202:S180–S186.

Nyangao J, Page N, Esona M, Peenze I, Gatheru Z, Tukei P, Steele AD. 2010. Characterization of human rotavirus strains from children with diarrhea in Nairobi and Kisumu, Kenya, between 2000 and 2002. J Infect Dis 202:S187–S192.

O'Halloran F, Lynch M, Cryan B, O'Shea H, Fanning S. 2000. Molecular characterization of rotavirus in Ireland: Detection of novel strains circulating in the population. J Clin Microbiol 38:3370–3374.

Paul SK, Kobayashi N, Nagashima S, Ishino M, Watanabe S, Alam MM, Ahmed MU, Hossain MA, Naik TN. 2008. Phylogenetic analysis of rotaviruses with genotypes G1, G2, G9 and G12 in Bangladesh: Evidence for a close relationship between rotaviruses from children and adults. Arch Virol 153:1999–2012.

Pietsch C, Petersen L, Patzer L, Liebert UG. 2009. Molecular characteristics of German G8P[4] rotavirus strain GER1H-09 suggest that a genotyping and subclassification update is required for G8. J Clin Microbiol 47:3569–3576.

Ramani S, Iturriza-Gomara M, Jana AK, Kuruvilla KA, Gray JJ, Brown DW, Kang G. 2009. Whole genome characterization of reassortant G10P[11] strain (N155) from a neonate with symptomatic rotavirus infection: Identification of genes of human and animal rotavirus origin. J Clin Virol 45:237–244.

Rao CD, Jagannath MR, Varshney BC, Das M, Reddy BSY. 2003. Genomic diversity through gene reassortment and antigenic drift and molecular epidemiology of rotaviruses in India. In: Kobayashi N, editor. Genomic diversity and molecular epidemiology of rotaviruses. Trivandrum. India: Research Signpost. pp 55–74.

Reidy N, Lennon G, Fanning S, Power E, O'Shea H. 2006. Molecular characterisation and analysis of bovine rotavirus strains circulating in Ireland 2002–2004. Vet Microbiol 117:242–247.

Saitou N, Nei M. 1987. The neighbor-joining method: A new method for reconstructing phylogenetic trees. Mol Biol Evol 4:406–425.

Salu OB, Audu R, Geyer A, Steele AD, Oyefolu AO. 2003. Molecular epidemiology of rotaviruses in Nigeria: Detection of unusual strains with G2P[6] and G8P[1] specificities. J Clin Microbiol 41:913–914.

Santos N, Hoshino Y. 2005. Global distribution of rotavirus serotypes/genotypes and its implication for the development and implementation of an effective rotavirus vaccine. Rev Med Virol 15:29–56.

Santos N, Lima RC, Pereira CF, Gouvea V. 1998. Detection of rotavirus types G8 and G10 among Brazilian children with diarrhea. J Clin Microbiol 36:2727–2729.

Steyer A, Poljsak-Prijatelj M, Bufon TL, Marcun-Varda N, Marin J. 2007. Rotavirus genotypes in Slovenia: Unexpected detection of G8P[8] and G12P[8] genotypes. J Med Virol 79:626–632.

Taniguchi K, Urasawa T, Morita Y, Greenberg HB, Urasawa S. 1987. Direct serotyping of human rotavirus in stools by an enzyme-linked immunosorbent assay using serotype 1-, 2-, 3-, and 4-specific monoclonal antibodies to VP7. J Infect Dis 155:1159–1166.

Taniguchi K, Urasawa T, Urasawa S, Yasuhara T. 1984. Production of subgroup-specific monoclonal antibodies against human rotaviruses and their application to an enzyme-linked immunosorbent assay for subgroup determination. J Med Virol 14:115–125.

Taniguchi K, Wakasugi F, Pongsuwanna Y, Urasawa T, Ukae S, Chiba S, Urasawa S. 1992. Identification of human and bovine rotavirus serotypes by polymerase chain reaction. Epidemiol Infect 109:303–312.

Tate JE, Rheingans RD, O'Reilly CE, Obonyo B, Burton DC, Tornheim JA, Adazu K, Jaron P, Ochieng B, Kerin T, Calhoun L, Hamel M, Laserson K, Breiman RF, Feikin DR, Mintz ED, Widdowson MA. 2009. Rotavirus disease burden and impact and cost-effectiveness of a rotavirus vaccination program in Kenya. J Infect Dis 200:S76–S84.

Tsugawa T, Hoshino Y. 2008. Whole genome sequence and phylogenetic analyses reveal human rotavirus G3P[3] strains Ro1845 and HCR3A are examples of direct virion transmission of canine/feline rotaviruses to humans. Virology 380:344–353.

Varghese V, Das S, Singh NB, Kojima K, Bhattacharya SK, Krishnan T, Kobayashi N, Naik TN. 2004. Molecular characterization of a human rotavirus reveals porcine characteristics in most of the genes including VP6 and NSP4. Arch Virol 149:155–172.

Varghese V, Ghosh S, Das S, Bhattacharya SK, Krishnan T, Karmakar P, Kobayashi N, Naik TN. 2006. Characterization of VP1, VP2 and VP3 gene segments of a human rotavirus closely related to porcine strains. Virus Genes 32:241–247.

JOURNAL OF VIROLOGY, Apr. 2010, p. 4002–4012
0022-538X/10/$12.00 doi:10.1128/JVI.02220-09

Vol. 84, No. 8

Rabies Virus Nucleoprotein Functions To Evade Activation of the RIG-I-Mediated Antiviral Response[▽]

Tatsunori Masatani,[1] Naoto Ito,[1,2] Kenta Shimizu,[1] Yuki Ito,[1] Keisuke Nakagawa,[1] Yoshiharu Sawaki,[3] Hiroyuki Koyama,[3] and Makoto Sugiyama[1,2]*

The United Graduate School of Veterinary Sciences, Gifu University, 1-1 Yanagido, Gifu 501-1193, Japan,[1] and Laboratory of Zoonotic Diseases[2] and Laboratory of Plant Cell Technology,[3] Faculty of Applied Biological Sciences, Gifu University, 1-1 Yanagido, Gifu 501-1193, Japan

Received 21 October 2009/Accepted 26 January 2010

The rabies virus Ni-CE strain causes nonlethal infection in adult mice after intracerebral inoculation, whereas the parental Nishigahara (Ni) strain kills mice. We previously reported that the chimeric CE(NiN) strain with the N gene from the Ni strain in the genetic background of the Ni-CE strain kills adult mice, indicating that the N gene is related to the different pathogenicities of Ni and Ni-CE strains. In the present study, to obtain an insight into the mechanism by which the N gene determines viral pathogenicity, we compared the effects of Ni, Ni-CE, and CE(NiN) infections on host gene expressions using a human neuroblastoma cell line. Microarray analysis of these infected cells revealed that the expression levels of particular genes in Ni- and CE(NiN)-infected cells, including beta interferon (IFN-β) and chemokine genes (i.e., CXCL10 and CCL5) were lower than those in Ni-CE-infected cells. We also demonstrated that Ni-CE infection activated the interferon regulatory factor 3 (IRF-3)-dependent IFN-β promoter and induced IRF-3 nuclear translocation more efficiently than did Ni or CE(NiN) infection. Furthermore, we showed that Ni-CE infection, but not Ni or CE(NiN) infection, strongly activates the IRF-3 pathway through activation of RIG-I, which is known as a cellular sensor of virus infection. These findings indicate that the N protein of rabies virus (Ni strain) has a function to evade the activation of RIG-I. To our knowledge, this is the first report that the *Mononegavirales* N protein functions to evade induction of host IFN and chemokines.

Rabies virus, which belongs to *Lyssavirus* of the family *Rhabdoviridae*, which belongs to the order *Mononegavirales*, is known as a highly neurotropic virus and causes fatal encephalitis accompanied by severe neurological symptoms in almost all mammals, including humans. The genome is an unsegmented negative sense RNA and contains five genes (N, P, M, G, and L genes) encoding nucleoprotein (N protein), phosphoprotein (P protein), matrix (M) protein, glycoprotein (G protein), and large (L) protein, respectively (12). The N, P, and L proteins form helical ribonucleoprotein (RNP), together with the viral genomic RNA. The N protein participates in encapsidation of the genomic RNA. Only the encapsidated genomic RNA can be a template for replication of the viral genome and transcription of the viral mRNAs by the RNA-dependent RNA polymerase, L protein. The P protein binds to both N and L proteins and functions as a cofactor of the viral RNA polymerase. During virus assembly, the RNP is wrapped into an envelope containing an inner layer of the M protein and the transmembrane spike protein, G protein.

In response to viral infection (e.g., picornavirus, bunyavirus, and flavivirus infections), neurons in the brain produce type I interferon (IFN) comprised of the IFN-α family and IFN-β, which induces an antiviral status of a cell and functions as a main player for the host innate immunity (8, 9). The brain neurons are also capable of responding to the produced type I IFN. The fact that rabies virus can efficiently replicate in brain neurons strongly suggests that the virus has a certain mechanism to circumvent the host innate immunity. Interestingly, it has recently been reported that the P protein counteracts the innate immunity by inhibiting the cellular IFN system (6, 7, 38, 39).

Recently, it has been reported that rabies virus infection is recognized by a cellular sensor protein, retinoic acid-inducible gene I (RIG-I), and then induces type I IFN (16). RIG-I contains two N-terminal caspase recruitment domains (CARDs) and a DExD/H-box helicase domain (43). The helicase domain of RIG-I recognizes viral RNAs, and their CARDs are responsible for signaling through interaction with IFN-β promoter stimulator 1 (IPS-1) (also known as MAVS, VISA, or CARDIF) (21). It has been proposed that RIG-I adopts a "closed (inactivated)" conformation in the absence of viral RNAs but changes to an "opened (activated)" structure upon binding to viral RNAs, exposing the CARDs (37). Interaction of RIG-I and IPS-1 results in activation of TANK-binding kinase 1 (TBK-1). Activated TBK-1 catalyzes phosphorylation and dimerization of interferon regulatory factor 3 (IRF-3). Dimerized IRF-3 is translocated into the nucleus, where, together with nuclear factor (NF)-κB, it activates the transcription of type I IFN (1, 14, 20). Brzozka et al. (6) reported that rabies virus P protein interferes with the phosphorylation of IRF-3 by TBK-1 and consequently inhibits type I IFN induction.

Type I IFN that is produced and secreted by infected cells interacts with its receptor on the cell surface and then activates JAK/STAT-medicated signal pathways that result in expression of antiviral proteins (1, 33). It has been reported that

* Corresponding author. Mailing address: Laboratory of Zoonotic Diseases, Faculty of Applied Biological Sciences, Gifu University, 1-1 Yanagido, Gifu 501-1193, Japan. Phone and fax: 81 58 293 2948. E-mail: sugiyama@gifu-u.ac.jp.

▽ Published ahead of print on 3 February 2010.

rabies virus P protein binds to STAT1 and STAT2, which are components of the transcription factor ISGF-3 for the type I IFN signaling pathway, and that the P protein inhibits the translocation of STAT1 and STAT2 to the nucleus and consequently suppresses cellular antiviral responses (7, 38, 39). As mentioned above, rabies virus P protein counteracts host innate immunity by inhibiting both type I IFN induction and cellular antiviral responses induced by IFN. On the other hand, the other protein of rabies virus that is responsible for circumvention of host innate immunity has not been reported yet.

The fixed rabies virus Nishigahara (Ni) strain kills adult mice after intracerebral (i.c.) inoculation, whereas the chicken embryo fibroblast cell-adapted strain Ni-CE causes nonlethal infection in adult mice (35). We have also reported that a chimeric virus, CE(NiN) strain, which has the N gene from Ni strain in the genetic background of Ni-CE strain, kills adult mice after i.c. inoculation. This indicated that the N gene is related to the different pathogenicities of Ni and Ni-CE strains. However, the mechanism by which the N gene from Ni strain determines the pathogenicity has not been clarified yet. In the present study, in order to obtain an insight into the mechanism, we comprehensively examined and compared the effects of Ni, Ni-CE, and CE(NiN) infections on host gene expressions of a human neuroblastoma cell line. DNA microarray analysis of these infected cells revealed that expression levels of particular genes in Ni and CE(NiN)-infected cells such as the IFN-β and chemokine genes, which are known to be regulated by IRF-3, were lower than the levels in Ni-CE-infected cells. Further analyses demonstrated that N protein of rabies virus (Ni strain) has a function to evade activation of the RIG-I-mediated antiviral response. To our knowledge, this is the first report that the *Mononegavirales* N protein functions to evade induction of host IFN and chemokines.

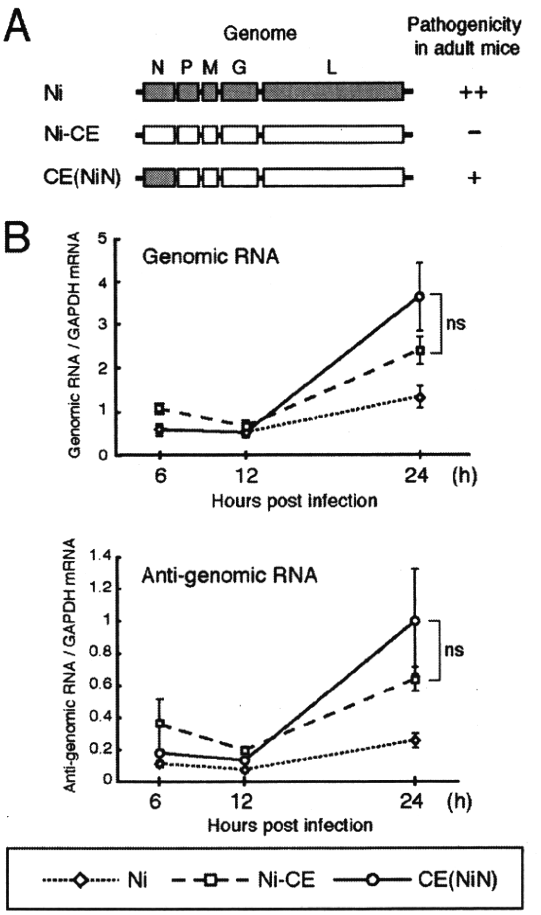

FIG. 1. Schematic diagrams of genome organizations and replication efficiency of Ni, Ni-CE, and CE(NiN) strains. (A) Schematic diagrams of genome organizations of Ni, Ni-CE, and chimeric CE(NiN) strains. Shaded and open boxes represent open reading frames derived from Ni and Ni-CE strains, respectively. The pathogenicity of each strain for adult mice determined by our previous study (35) is also indicated. The pathogenicity was previously evaluated by i.c. inoculation with 1,000 FFU of each virus. ++, Lethal (all mice died within 7 days); +, lethal (all mice died within 10 days); −, nonlethal. (B) SYM-I cells were infected with Ni, Ni-CE, and CE(NiN) strains at an MOI of 2. Total cellular RNA was extracted at 6, 12, and 24 hpi and analyzed for viral genomic and antigenomic RNA levels by real-time PCR. Expression levels of genes were normalized to mRNA levels of *GAPDH*. Each point represents the mean (± the SD) of three independent replicates. ns, no significant difference.

MATERIALS AND METHODS

Cells and viruses. Human neuroblastoma SYM-I cells (kindly provided by A. Kawai) (15) and mouse neuroblastoma NA cells were maintained in Eagle minimal essential medium supplemented with 10% fetal calf serum. 293T cells were maintained in Dulbecco minimal essential medium (high glucose) supplemented with 10% fetal calf serum. Recombinant Ni and Ni-CE strains were recovered from the cloned cDNA of the respective strains, as reported previously (35, 42). The chimeric CE(NiN) strain was previously generated by using the reverse genetic system of Ni-CE strain (35). The genomic organizations of Ni, Ni-CE, and CE(NiN) strains and their pathogenicities for adult mice are shown in Fig. 1A. Stocks of all rabies virus strains were prepared in NA cells. The B-1 vaccine strain of Newcastle disease virus (NDV) was kindly provided by H. Fukushi. NDV was grown in 10-day-old embryonated chicken eggs.

Propagation of Ni, Ni-CE, and CE(NiN) strains in SYM-I cells. SYM-I cells grown in a 24-well tissue culture plate (Greiner Bio-One Co., Ltd) were inoculated with Ni, Ni-CE, and CE(NiN) strains at a multiplicity of infection (MOI) of 2. At 24 h postinfection (hpi), viruses in the culture supernatants were harvested and titrated in NA cells by indirect focus assay using monoclonal antibody 13-27 specific for N protein (27).

Total RNA preparation. A monolayer culture of SYM-I cells was infected with each rabies virus at an MOI of 2. Total cellular RNA was extracted at 6, 12, and 24 hpi using an RNeasy Mini Total RNA extraction kit (Qiagen). The extracted RNA was treated with an RNase-free DNase kit (Qiagen) and suspended in nuclease-free water. RNA preparations used for DNA microarray analysis were analyzed with a lab-on-a-chip Agilent Bioanalyzer (RNA 6000 LabChip kit; Agilent) to confirm the concentration, integrity, and purity.

DNA microarray hybridization and analysis. cRNA used for DNA microarray hybridization was prepared according to the One-Color microarray-based gene expression analysis protocol (Agilent). Probes were synthesized from 600 ng of total RNA isolated from two independent biological replicates in two steps according to the manufacturer's instructions. In the first step, double-stranded cDNA was synthesized with mouse Moloney murine leukemia virus reverse transcriptase (Agilent) and an oligo(dT)-T7 RNA polymerase promoter (Agilent). In the second step, we synthesized antisense cRNAs that were labeled by the incorporation of Cy3-CTP during *in vitro* transcription. All reagents were from Agilent's fluorescent linear amplification kit adapted for use with small amounts of total RNA. Labeled cRNAs were fragmented to an average size of 50 to 100 nucleotides by heating the samples at 60°C in a fragmentation buffer provided by Agilent. Hybridization was performed on whole-human-genome 4 × 44K oligonucleotide microarrays (G4112F; Agilent) with reagents and protocols provided by the manufacturer. After hybridization, the arrays were washed and scanned using a DNA microarray scanner (Agilent). Feature extraction software provided by Agilent (version 9.1) was used to quantify the intensity of fluorescent images and to normalize results by subtracting local background fluorescence, according to the manufacturer's instructions. The expression level of each gene was analyzed by GeneSpring GX software (version 7.3.1; Agilent). Briefly, after

TABLE 1. Sequences of the primers and TaqMan probe

Analysis	Primer or probe	Sequence (5′→3′)
RT	Rabies RT for genome	CTGCTTGTAAACCAGGCATTCCCGGATGTCTG
	Rabies RT for anti-genome	AAACAATCAAACAGCCAGAGGTCCAGATTC
SYBR green assay	Human GAPDH F	CCTCCTGTTCGACAGTCAGC
	Human GAPDH R	CGCCCAATACGACCAAATC
TaqMan assay	Rabies TaqMan probe	TGATGTGTCTCGAAAA
	Rabies genome F	GTCTGCACATGCTGAGACTCTTG
	Rabies genome R	ACAGCCAGAGGTCCAGATTCA

importing the processed data into the software, they were normalized based on the default normalizing settings for one-color experiments (GeneSpring 7.3 user's guide; Agilent). Cluster analysis was performed by using Cluster 3.0 and Java TreeView.

Real-time reverse transcription-PCR (RT-PCR). To measure levels of virus genomic and antigenomic RNAs in infected cells, total RNA was reverse transcribed into cDNAs by using SuperScript III reverse transcriptase (Invitrogen) with reverse transcriptase primers specific to rabies virus genomic and antigenomic RNAs (Table 1) or oligo(dT)$_{20}$ [for detection of human housekeeping glyceraldehyde 3-phosphate dehydrogenase (GAPDH) mRNA, Invitrogen]. Real-time PCR was performed by using an ABI 7300 real-time PCR system (Applied Biosystems) and TaqMan 2×PCR Universal Master Mix (for detection of virus genomic and antigenomic RNA; Applied Biosystems) or SYBR Premix Ex Taq II (for detection of human GAPDH mRNA; TaKaRa Bio). PCR conditions were as follows: 50°C for 2 min, 95°C for 10 min, and 40 cycles of 95°C for 15 s and 60°C for 1 min (TaqMan assay) or 95°C for 10 s and 40 cycles of 95°C for 5 s and 60°C for 31 s (SYBR green assay). To detect virus genomic and antigenomic RNAs, we used primers and a TaqMan probe set that corresponded to the trailer sequence of rabies virus genomic RNA, which is conserved between Ni and Ni-CE strains. Sequences of the primers and a TaqMan probe are shown in Table 1.

For validation of microarray data, total RNA was reverse transcribed into cDNAs using SuperScript III reverse transcriptase and random hexamer (TaKaRa Bio). Primer and probe sets for relative quantification of human genes were selected from the product list of TaqMan gene expression assays (Applied Biosystems). A TaqMan assay was performed as described above.

Data are expressed as number of copies of specific mRNA per copy of human GAPDH mRNA. All assays were carried out in triplicate and the results are expressed as means ± the standard deviation (SD).

Plasmids. Using conventional cloning techniques, we subcloned a PCR-amplified cDNA fragment of the full-length N gene from Ni or Ni-CE strain into a polymerase II-based expression plasmid, pCAGGS/MCS (kindly provided by Y. Kawaoka) and named the respective resulting plasmids pCAGGS-NiN and -CEN. Similarly, we constructed pCAGGS-NiP and -CEP plasmids expressing Ni and Ni-CE P protein, respectively. Details of the construction of these plasmids and sequences of primers are available from the authors on request. 4×IRF-3-Luc (kindly provided by S. Ludwig) (11) contains four copies of the IRF-3-binding positive regulatory domain (PRD) I/III motif of the IFN-β promoter upstream of the luciferase reporter gene. pNF-κB-Luc (Stratagene) contains five copies of the NF-κB-binding motif of the IFN-β promoter upstream of the luciferase reporter gene. pRL-TK (Promega), used as an internal control for the reporter assay, contains the *Renilla* luciferase gene downstream of the herpes simplex virus thymidine kinase promoter that is activated in mammalian cells. pEGFP-C1-hIRF-3 (kindly provided by C. F. Basler) (5) express the human IRF-3 protein fused to green fluorescent protein (GFP-IRF-3). Expression plasmids for wild-type RIG-I (pEF-Flag-RIG-I), constitutively active mutant (pEF-Flag-RIG-IN), dominant-negative mutant (pEF-Flag-RIG-IC), wild-type IPS-1 (pEF-Flag-IPS-1), and empty plasmid [pEF-BOS(+)] were kindly provided by T. Fujita (24, 43).

Transfection and reporter assay. Transfection was performed by using Lipofectamine 2000 (Invitrogen) according to the manufacturer's instructions. SYM-I cells were transfected with 1 μg of viral N or P protein-expressing plasmids or pEF-Flag-RIG-I, 0.25 μg of 4×IRF-3-Luc or pNF-κB-Luc, and 0.04 μg of pRL-TK. At 24 hpi, cells were infected with Ni, Ni-CE, or CE(NiN) strains (MOI of 2) or NDV (MOI of 1). In another series of experiments, SYM-I cells were inoculated, in suspension, with Ni, Ni-CE, or CE(NiN) strain at an MOI of 2 and seeded in a 24-well tissue culture plate at 2×10^5 cells per well. At 24 hpi, cells were transfected with 0.5, 1, or 2 μg of pEF-Flag-RIG-IC or 1 μg of pEF-Flag-RIG-IN in addition to 0.25 μg of 4×IRF-3-Luc and 0.04 μg of pRL-TK.

At the completion of the experiments, cells were lysed, and the activities of firefly and *Renilla* luciferases were determined by a dual-luciferase reporter assay system (Promega) according to the manufacturer's instructions. The data represent firefly luciferase activity normalized to *Renilla* luciferase activity. All assays were carried out in triplicate, and the results expressed as means ± the SD.

IRF-3 nuclear translocation assay. SYM-I cells were inoculated, in suspension, with Ni, Ni-CE, or CE(NiN) strain at an MOI of 2 and seeded in a 24-well tissue culture plate at 2×10^5 cells per well. At 24 hpi, cells were transfected with 1 μg of pEGFP-C1-hIRF-3 using Lipofectamine 2000. At 24 h posttransfection, cells were fixed in 4% paraformaldehyde for 60 min and 100% methanol for 1 min. Then, infected cells were stained with anti-N protein mouse monoclonal antibody 13-27 and then TRITC-goat anti-mouse IgG (H+L) conjugate (Zymed). The localization of GFP-IRF-3 was examined with a Biozero fluorescence microscope (BZ-8000 series; Keyence). The percentage of virus-infected cells with nuclear GFP-IRF-3 localization was then determined by counting 100 infected cells. The results are expressed as means ± the SD of three independent wells.

Immunofluorescence staining. Confluent SYM-I cells were grown in a 24-well plate and inoculated with Ni, Ni-CE, or CE(NiN) strain at an MOI of 2. At 24 hpi, cells were fixed with 4% paraformaldehyde for 60 min and 100% methanol for 1 min. The fixed cells were double stained by using anti-N protein mouse monoclonal antibody 13-27 and anti-human IRF-3 rabbit polyclonal antibody FL-425 (Santa Cruz) as primary antibodies and using TRITC (tetramethyl rhodamine isothiocyanate)-goat anti-mouse IgG (H+L) Conjugate and fluorescein isothiocyanate (FITC)-goat anti-rabbit IgG (Cappel) as secondary antibodies. Fluorescence was visualized by using a Biozero fluorescence microscope.

Western blotting. Cells were lysed in lysis buffer (50 mM Tris-HCl [pH 7.5], 150 mM NaCl, 1 mM EDTA, 1% NP-40) supplemented with 0.02 mM *p*-amidinophenylmethanesulfonyl fluoride at 24 hpi, and the samples were incubated on ice for 15 min. After centrifugation (15,000 × *g*, 10 min, 4°C), the soluble fractions were separated electrophoretically on 10% sodium dodecyl sulfate (SDS)-polyacrylamide gels and transferred to polyvinylidene difluoride membranes (Millipore). The membranes were blocked with phosphate-buffered saline (PBS) containing 0.1% Tween 20 and 5% nonfat dry milk. The following antibodies were used to probe the blots: anti-N protein mouse monoclonal antibody 13-27, anti-P protein rabbit polyclonal antibody (kindly provided by A. Kawai), anti-Flag rabbit polyclonal antibody (Sigma), and anti-α-tubulin monoclonal antibody (Sigma). Antibody signals were detected by chemiluminescence using horseradish peroxidase (HRP)-conjugated anti-rabbit IgG (H+L; Seikagaku Corp.) or HRP-conjugated anti-mouse IgG (Fab2; Cappel) and a Western Lightning Plus ECL kit (Perkin-Elmer). Chemiluminescent signals were detected and visualized by using a LAS-1000 Lumino image analyzer (Fuji Film). Densitometry analysis was carried out by using ImageJ software. Briefly, the intensity of images of scanned Western blots was determined, and the ratio of each band to its tubulin control was calculated.

IRF-3 dimerization analysis. SYM-I cells grown in a six-well tissue culture plate were inoculated with Ni, Ni-CE, or CE(NiN) strain at an MOI of 10. Cells were lysed in the lysis buffer described above, which was supplemented with Complete mini-protease inhibitor cocktail (Roche) at 24 hpi, and the samples were incubated on ice for 15 min. After centrifugation (15,000 × *g*, 10 min, 4°C), the soluble fractions were separated electrophoretically on a 7.5% Ready Gels J (Bio-Rad), with 1% deoxycholate in the cathode buffer (25 mM Tris-HCl [pH 8.4], 192 mM glycine). IRF-3 was detected by using Western blotting with polyclonal anti-IRF-3 (Santa Cruz) and HRP-conjugated anti-rabbit IgG (H+L; Seikagaku Corp.).

Coimmunoprecipitation analysis. SYM-I cells in a six-well plate were cotransfected with 4 μg of pCAGGS-CEP and 4 μg of pCAGGS-NiN or pCAGGS-

TABLE 2. Number and percentage of host genes affected by infection of each virus

Strain	No. (%) of host genes affected[a]		
	Upregulation	Downregulation	Total
Ni	241 (0.59)	76 (0.19)	317 (0.77)
Ni-CE	765 (1.86)	113 (0.27)	878 (2.14)
CE(NiN)	628 (1.53)	130 (0.32)	758 (1.85)

[a] A total of 41,063 genes were analyzed. A gene was considered differentially expressed if the expression level was 3-fold higher or lower than the level in mock-infected cells.

CEN. After the cells were washed with PBS at 48 h posttransfection, cell extracts were prepared by lysing cells on ice for 15 min in TN buffer (50 mM Tris-HCl [pH 8.4], 150 mM NaCl) containing 1% NP-40 and protease inhibitor (Complete mini; Roche). Lysates were centrifuged at 15,000 × *g* for 10 min at 4°C to remove large debris. Protein A/G Plus-Agarose (Santa Cruz) was incubated with anti-N protein mouse monoclonal antibody 13-27 or mouse normal IgG (Sigma) for 2 h at room temperature and then washed three times with TN buffer containing 1% NP-40 and protease inhibitor. Lysates were incubated with agarose beads overnight with rotation at 4°C. The agarose beads were washed five times with TN buffer containing 1% NP-40 and protease inhibitor and boiled with SDS sample buffer for 5 min. The supernatant of the agarose was subjected to SDS-polyacrylamide gel electrophoresis (PAGE) and Western blotting.

Statistical analysis. A Student *t* test was used to determine statistical significance, and *P* values of <0.01 were considered statistically significant.

RESULTS

Genome replication and viral growth of Ni, Ni-CE, and CE(NiN) strains in SYM-I cells. In order to obtain insights into the mechanism by which the N gene determines viral pathogenicity, we tried to comprehensively compare the gene expressions of host cells infected with Ni, Ni-CE, and CE(NiN) strains using a DNA microarray. Human neuroblastoma SYM-I cells are known to be susceptible to rabies virus and to produce IFN-β in response to viral infection (15). Therefore, this cell line is suitable for examining the effects of rabies virus infection on the expression of host genes, especially genes related to host innate immunity.

First, we measured levels of viral genomic and antigenomic RNAs in SYM-I cells infected with Ni, Ni-CE, and CE(NiN) strains at 6, 12, and 24 hpi using quantitative real-time RT-PCR (Fig. 1B). The amount of genomic RNA of each strain increased markedly between 12 and 24 hpi (Fig. 1B top), indicating genome replication in this cell line. We found that genome replication of Ni strain was less efficient than that of Ni-CE and CE(NiN) strains, probably due to the fact that Ni strain has been maintained by rabbit brain passages (17) and is not well adapted to cultured cells. In contrast, there was no significant difference in the amount of genomic RNA between Ni-CE- and CE(NiN)-infected cells at 24 hpi. Similar kinetics was observed in antigenomic RNA in the cells infected with each strain (Fig. 1B, bottom).

Next, we examined growth of Ni, Ni-CE, and CE(NiN) strains in SYM-I cells at 24 hpi. Consistent with the viral RNA replication, virus titers of Ni-CE and CE(NiN) strains in the culture media were almost identical (9.7×10^3 and 1.6×10^4 focus-forming units [FFU]/ml, respectively), whereas the titer of Ni strain (4.4×10^3 FFU/ml) was ~2-fold lower than that of Ni-CE and CE(NiN) strains. Hence, we chose 24 hpi as the condition for DNA microarray analysis, in order to minimize the influence of replication efficiencies of Ni-CE and CE(NiN) strains.

DNA microarray analysis of SYM-I cells infected with Ni, Ni-CE, and CE(NiN) strains. We successfully collected normalized data for 40,613 human genes by the DNA microarray analysis. We considered a gene to be differently expressed if the expression level was 3-fold higher or lower than the level in mock-infected cells. The total number of genes affected by Ni-CE infection (878 genes) was much larger than that affected by Ni infection (317 genes) (Table 2). This was mainly due to the difference between numbers of upregulated genes in the Ni- and Ni-CE-infected cells (241 and 765 genes, respectively). On the other hand, the number of upregulated genes in CE(NiN)-infected cells (628 genes) was very similar to that in Ni-CE-infected cells.

To focus on the genes related to host immunity, we carried out cluster analysis using a bioset that contained a selection of genes involved in "host-pathogen interaction" (GO accession number 0030383, 1,722 genes) (Fig. 2A). The gene expression pattern of Ni-CE-infected cells was more similar to that of CE(NiN)-infected cells than to that of Ni-infected cells:

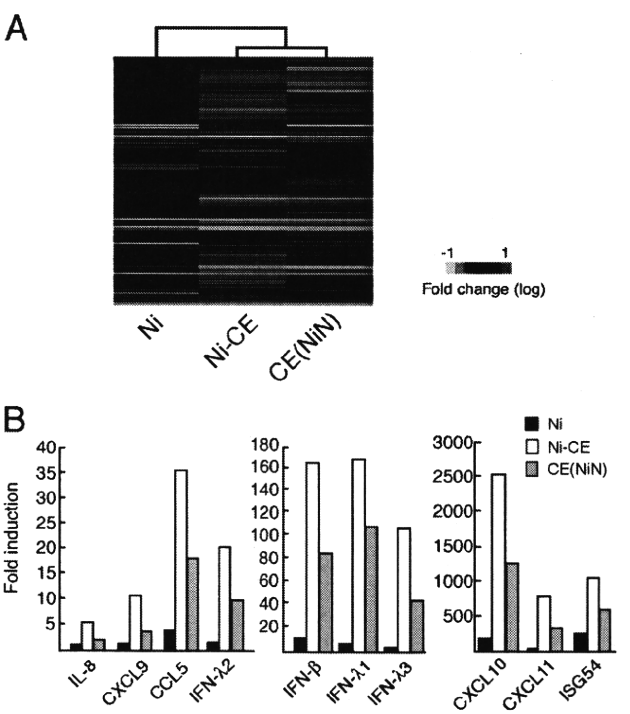

FIG. 2. Comparison of the gene expressions of SYM-I cells infected with Ni, Ni-CE, and CE(NiN) strains using a DNA microarray. SYM-I cells were infected with Ni, Ni-CE, and CE(NiN) strains at an MOI of 2. After 24 h, the total cellular RNA was extracted and used for DNA microarray analysis. The data were normalized by Gene Spring GX software. (A) Cluster analysis of genes of SYM-I cells infected with each virus. The expression pattern of genes involved in "host-pathogen interaction" is represented as a hierarchical clustering, using Cluster and Java TreeView. Genes shown in red are upregulated, and those shown in green are downregulated relative to mock-infected cells. (B) Expression levels of 10 host immunity-related genes, most of which were differentially expressed in Ni-CE- and CE(NiN)-infected cells. Each bar represents the fold change in expression compared to the expression level of each gene in mock-infected cells.

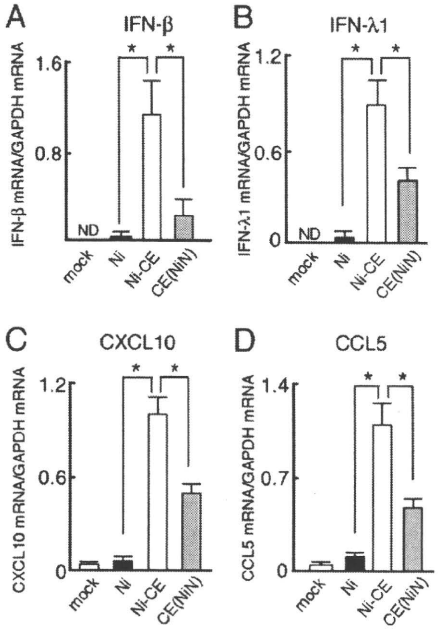

FIG. 3. Validation by real-time RT-PCR of DNA microarray results for *IFN-β* (A), *IFN-λ1* (B), *CXCL10* (C), and *CCL5* (D). The assay was performed with the same total RNA used in the DNA microarray experiment. Expression levels of genes were normalized to mRNA levels of *GAPDH*. Each bar represents the mean (± the SD) of three independent replicates. *, Significant difference ($P < 0.01$); ND, no detection.

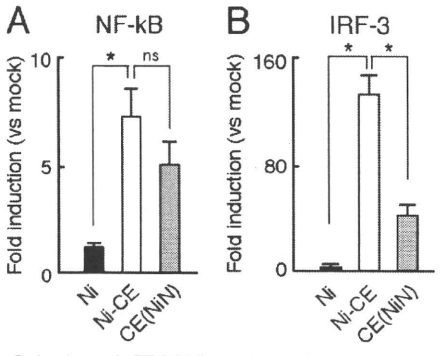

FIG. 4. Infection of CE(NiN) strain inhibits activation of IRF-3-dependent but not NF-κB-dependent IFN-β promoter. SYM-I cells were cotransfected with pRL-TK and pNF-κB-Luc (NF-κB-responsive reporter plasmid) (A) or 4×IRF-3-Luc (IRF-3-responsive reporter plasmid) (B). After 24 h, the cells were mock infected or infected with each strain at an MOI of 2. The luciferase activities were measured 24 h after transfection. The data represent firefly luciferase activity normalized to *Renilla* luciferase activity and are presented as means (± the SD) of three independent replicates. *, Significant difference ($P < 0.01$); ns, no significant difference.

changes in gene expression in Ni-CE- and CE(NiN)-infected cells were more drastic than those in Ni-infected cells. Similar results were obtained by using a bioset of "defense immunity protein activity" (GO accession number 0003793, 1,011 genes) (data not shown).

Although overall gene expression patterns of Ni-CE- and CE(NiN)-infected cells were very similar as mentioned above, the expression levels of a part of the host genes were clearly different in Ni-CE- and CE(NiN)-infected cells. For example, expression level of the *IFN-β* gene in Ni-CE-infected cells was 2-fold higher than the level in CE(NiN)-infected cells (Fig. 2B). Similar results were obtained for the gene expression levels of type III IFN (*IFN-λ1*, *IFN-λ2*, and *IFN-λ3*); *ISG54*, which is known to be IFN-inducible (29); and chemokines (*CXCL9*, *CXCL10*, and *CXCL11*; *CCL5*; and *IL-8*) (Fig. 2B). Since Ni-CE and CE(NiN) strains genetically differ only in the N gene, we considered that the different gene expressions of Ni-CE- and CE(NiN)-infected cells were due to functional difference in the N gene. Notably, expression levels of these host genes in Ni-infected cells were much lower than those in Ni-CE- and CE(NiN)-infected cells (Fig. 2B).

Validation of microarray data by using quantitative real-time RT-PCR. To confirm the different gene expression patterns of Ni-, Ni-CE-, and CE(NiN)-infected cells that were revealed by DNA microarray analysis, we quantified *IFN-β*, *IFN-λ1*, *CXCL10*, and *CCL5* mRNAs in these infected cells by using quantitative real-time RT-PCR (Fig. 3). Corresponding to the DNA microarray data, expression level of the *IFN-β* gene in Ni-CE-infected cells was 40- and 4-fold higher than the levels in Ni- and CE(NiN)-infected cells, respectively (Fig. 3A). Similarly, it was shown that Ni-CE infection induced the expression of *IFN-λ1*, *CXCL10*, and *CCL5* genes more efficiently than did Ni and CE(NiN) infections (Fig. 3B, C, and D, respectively). These results clearly showed that the Ni N gene functions to suppress expression of innate immunity and inflammatory genes in infected host cells.

Identification of the signaling pathway involved in the suppressed expressions of IFN and chemokine genes by Ni N gene. Expressions of *IFN-β*, *IFN-λ*, and chemokine genes have been shown to be regulated by the transcription factors NF-κB and IRF-3, which are activated by the respective upstream signaling pathway (13, 14, 23, 29, 30, 40). In order to identify the signaling pathway that is involved in the suppressed expressions of *IFN-β* gene in Ni- and CE(NiN)-infected cells, we measured NF-κB- or IRF-3-dependent IFN-β promoter activities in Ni-, Ni-CE-, and CE(NiN)-infected cells by luciferase-based reporter assays with reporter plasmids having the NF-κB- or IRF-3-binding site (PRD II or PRD I/III, respectively) of the IFN-β promoter (Fig. 4). Although NF-κB-dependent IFN-β promoter activity in Ni-infected cells was significantly lower than that in Ni-CE-infected cells ($P < 0.01$), there was no difference between the activities in Ni-CE- and CE(NiN)-infected cells (Fig. 4A). In contrast, IRF3-dependent IFN-β promoter activities in Ni- and CE(NiN)-infected cells (4- and 38-fold inductions, respectively) were significantly lower than that in Ni-CE-infected cells (126-fold induction) ($P < 0.01$) (Fig. 4B). These results indicated that the IRF-3 pathway, rather than the NF-κB pathway, is involved in suppressed expression of the *IFN-β* gene in Ni- and CE(NiN)-infected cells.

Subcellular localization and dimerization of IRF-3 in SYM-I cells infected with each virus. In order to check subcellular localization of IRF-3 in infected cells, we transfected pEGFP-C1-hIRF-3 expressing GFP-IRF-3 into Ni-, Ni-CE-, and CE(NiN)-infected cells (Fig. 5A). We also determined the percentage of infected cells with nuclear GFP-IRF-3 in GFP-

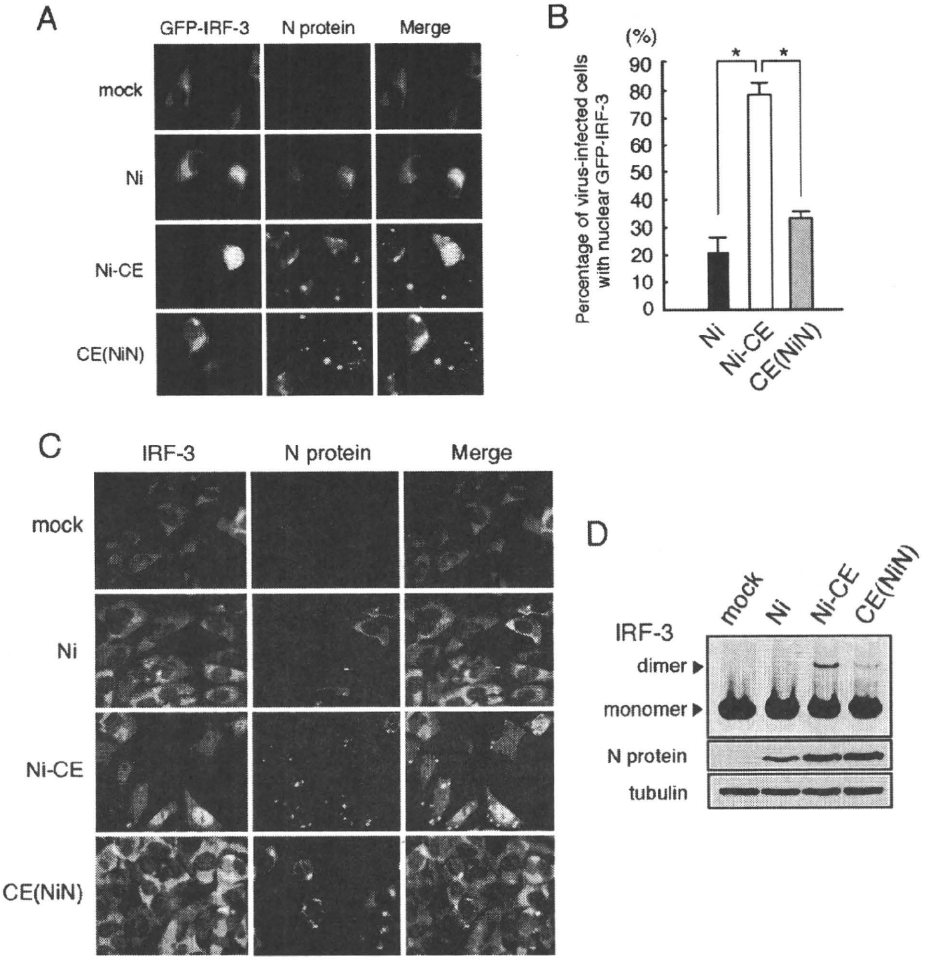

FIG. 5. Ni and CE(NiN) infections prevent nuclear translocation and dimerization of IRF-3. (A) SYM-I cells were inoculated, in suspension, with each virus strain at an MOI of 2 FFU/cells and seeded. After 24 h, cells were transfected with the GFP-IRF-3 expression plasmid (green). At 24 h posttransfection, the cells were fixed and stained with an anti-N monoclonal antibody (red). (B) Assessment of the rate of GFP-IRF-3 nuclear translocation in GFP-IRF-3-expressing and virus-infected calls. Each value is the average (± the SD) of three independent experiments in which 100 cells were counted. *, Significant difference ($P < 0.01$). (C) Subcellular localization of endogenous IRF-3 in SYM-I cells infected with each strain. SYM-I cells were mock infected or infected with Ni, Ni-CE, or CE(NiN) strains at an MOI of 2. After 24 h, cells were fixed and examined by double immunofluorescence staining using anti-IRF-3 polyclonal antibody (green) and anti-N monoclonal antibody (red). (D) Extracts from SYM-I cells infected with Ni, Ni-CE, and CE(NiN) strains for 24 h were analyzed by native gel electrophoresis, followed by Western blotting, to detect IRF-3. N protein and tubulin of same samples were detected by SDS-PAGE, followed by Western blotting.

positive infected cells (Fig. 5B). In mock-infected cells, GFP-IRF-3 was localized in the cytoplasm, whereas the signals in Ni-CE-infected cells were observed mainly in the nucleus. It was shown that 79% of GFP-positive Ni-CE-infected cells had the signal in the nucleus. In contrast, in Ni- and CE(NiN)-infected cells, GFP-IRF-3 was localized mainly in the cytoplasm: only 22% of GFP-positive Ni-infected cells and 33% of CE(NiN)-infected cells had signals in the nucleus. Similar results were obtained by immunostaining of endogenous IRF-3 in Ni-, Ni-CE-, and CE(NiN)-infected cells (Fig. 5C). These results indicated that Ni and CE(NiN) infections suppress translocation of IRF-3 to the nucleus or the upstream signaling pathway. We next examined the IRF-3 homodimerization in Ni-, Ni-CE-, and CE(NiN)-infected cells by native-PAGE (Fig. 5D). In contrast to Ni-CE-infected cells, in which a prominent band of IRF-3 dimers was detectable, dimerization of IRF-3 was suppressed in Ni- and CE(NiN)-infected cells. Taken together, these results indicated that Ni and CE(NiN) infection suppress the dimerization of IRF-3 and subsequent translocation of IRF-3 to the nucleus.

Ni N protein functions to evade activation of the IRF-3 pathway in the presence of other viral components. To determine whether single expression of Ni N protein is sufficient to inhibit the IRF-3 pathway, we checked IRF-3-dependent IFN-β promoter activities in Ni N protein- or Ni-CE N protein-expressing SYM-I cells after inoculation of NDV, which is known as a type I IFN inducer (18). Since single expression of rabies virus P protein is known to inhibit the IRF-3 pathway (6), we also expressed Ni P protein as a positive control. In contrast to expression of Ni P protein that inhibited IRF-3-dependent IFN-β promoter activity in NDV-infected cells, neither single expression of Ni nor Ni-CE N protein inhibited the

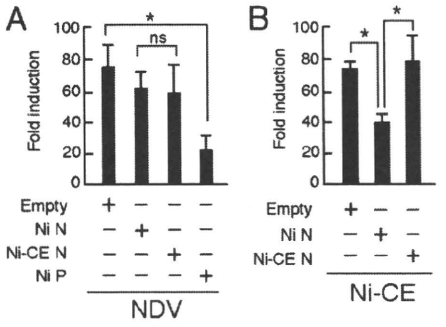

FIG. 6. Effects of transient expression of Ni or Ni-CE N protein on IRF-3-dependent promoter activities in SYM-I cells infected with NDV or Ni-CE strain. SYM-I cells were cotransfected with pRL-TK, 4×IRF-3-Luc, and 1 μg of each plasmid driving the expression of the indicated viral protein or empty vector. At 24 h posttransfection, the cells were infected with NDV at an MOI of 1 and incubated for 12 h (A) or infected with Ni-CE strain at an MOI of 2 and incubated for 24 h (B). Then, the cells were lysed, and the luciferase activities were measured. The data represent firefly luciferase activity normalized to *Renilla* luciferase activity and are presented as means (± the SD) of three independent replicates. *, Significant difference ($P < 0.01$); ns, no significant difference.

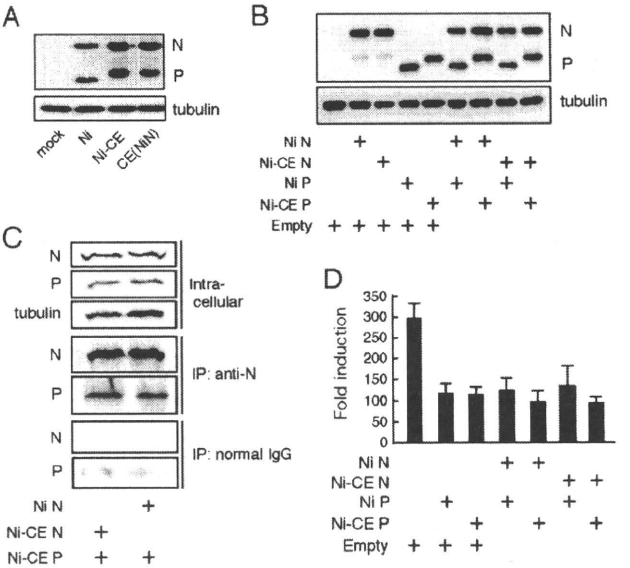

FIG. 7. N protein does not affect expression level of and activity of viral P protein to inhibit the IRF-3 pathway. (A) SYM-I cells were infected with the Ni, Ni-CE, or CE(NiN) strain at an MOI of 2. After 24 h, the cells were lysed and N, P, and tubulin were detected by Western blotting. (B) SYM-I cells in a 24-well plate were cotransfected with 1 μg of each plasmid driving the expression of the indicated viral protein or empty vector. At 48 h posttransfection, the cells were lysed, and N, P, and tubulin were detected by Western blotting. (C) SYM-I cells in a six-well plate were cotransfected with 4 μg of pCAGGS-CEP and 4 μg of pCAGGS-NiN or pCAGGS-CEN. Cell extracts were prepared at 48 h posttransfection and directly subjected to Western blotting with anti-N antibody, anti-P antibody, or anti-tubulin antibody (top). The same cell extracts were subjected to coimmunoprecipitation analysis with anti-N antibody (middle) or normal mouse IgG (bottom). The immunoprecipitated samples were examined by Western blotting. (D) SYM-I cells were cotransfected with pRL-TK, 4×IRF-3-Luc, and 1 μg of each plasmid driving the expression of the indicated viral protein or empty vector. At 24 h posttransfection, the cells were infected with NDV at an MOI of 1 and incubated for 12 h. Then the cells were lysed and luciferase activities were measured. The data represent firefly luciferase activity normalized to *Renilla* luciferase activity and are presented as means (± the SD) of three independent replicates.

promoter activity (Fig. 6A). There was no significant difference between the activities of Ni N protein- and Ni-CE N protein-expressing cells. Similar results were obtained by using transfection of a double-stranded RNA homolog, poly(I:C), instead of NDV infection, as an IFN inducer (data not shown). These results indicated that single expression of Ni N protein does not inhibit the IRF-3 pathway and strongly suggested that other rabies viral components are required to evade activation of the IRF-3 pathway by Ni N protein.

To determine whether other rabies viral components are involved in the evasion of activation of the IRF-3 pathway by the N protein, we inoculated Ni-CE strain as an IFN inducer into Ni N protein- or Ni-CE N protein-expressing SYM-I cells and then checked the IRF-3-dependent IFN-β promoter activities (Fig. 6B). The promoter activity induced by Ni-CE infection was significantly lower in Ni N protein-expressing cells than the activity in the empty vector-transfected cells ($P < 0.01$). In contrast, overexpression of Ni-CE N protein did not affect the promoter activity: the activity in Ni-CE N protein-expressing cells was significantly higher than the activity in Ni N protein-expressing cells ($P < 0.01$). These results indicated that Ni N protein, but not Ni-CE N protein, functions to evade activation of the IRF-3 pathway in the presence of other viral components.

N protein does not affect expression level and activity of viral P protein to inhibit the IRF-3 pathway. Rabies virus N protein is known to physically interact with the P protein (12, 26), which is known to inhibit type I IFN induction by inhibiting phosphorylation of IRF-3 by TBK-1 (6). Therefore, we hypothesized that Ni and Ni-CE N proteins would differently affect the N-P interaction and, consequently, would alter the expression levels or biological property of P protein. First, we examined expression levels of P proteins in Ni-, Ni-CE-, and CE(NiN)-infected cells by using Western blotting. We found that the expression levels of both N and P proteins in Ni-infected cells were lower than the levels of the respective protein in Ni-CE- and CE(NiN)-infected cells (Fig. 7A), reflecting the lower propagation efficiency of Ni strain described above. Also, the band mobility of Ni P protein was found to be slightly faster than that of Ni-CE P protein, probably due to the conformational differences of the Ni and Ni-CE P proteins. Importantly, we did not observe a clear difference between expression levels of P protein in Ni-CE- and CE(NiN)-infected cells. Consistent with this result, coexpression of Ni or Ni-CE N protein and P protein did not affect the expression levels of P protein from both strains (Fig. 7B). These results demonstrated that Ni and Ni-CE N proteins do not differently affect the expression level of P protein. Furthermore, to compare binding abilities of Ni and Ni-CE N proteins to Ni-CE P protein, we carried out coimmunoprecipitation analysis (Fig. 7C). Lysates of SYM-I cells coexpressing Ni-CE P protein and each of Ni and Ni-CE N proteins were subjected to IP with an anti-N protein monoclonal antibody or normal IgG. Both Ni and Ni-CE N proteins were detected in the precipitates after immunoprecipitation with an anti-N antibody (Fig. 7C, mid-

dle) but not after immunoprecipitation with normal mouse IgG (Fig. 7C, bottom), indicating that the anti-N antibody specifically binds to the N proteins. Notably, both precipitates that contained Ni and Ni-CE N proteins included comparable amounts of Ni-CE P protein (Fig. 7C, middle). The data indicated that both Ni and Ni-CE N proteins bind to Ni-CE P protein with similar efficiency.

Next, in order to test whether Ni N protein, but not Ni-CE N protein, enhances inhibitory activity of P protein on the IRF-3 pathway, we measured IRF-3-dependent IFN-β promoter activities in NDV-infected SYM-I cells coexpressing Ni or Ni-CE N and P proteins in different combinations (Fig. 7D). Single expression of Ni and Ni-CE P proteins equally inhibited activation of the IFN-β promoter induced by NDV infection. Importantly, we found that coexpression of Ni- or Ni-CE N and P proteins in any combinations did not affect the inhibitory activity of the respective P protein on the IRF-3 pathway.

Ni N protein, but not Ni-CE N protein, functions to evade activation of RIG-I-mediated antiviral response. Rabies virus N protein is also known to physically interact with the viral genomic RNA (2–4). It was previously reported that genomic RNA of rabies virus is recognized by RIG-I and induces type-I IFN production (16). Hence, we hypothesized that Ni N protein, but not Ni-CE N protein, functions to inhibit recognition of viral genomic RNA by RIG-I. First, to investigate the effect of infection of each virus on the RIG-I-mediated IRF-3 pathway, we transfected a wild-type RIG-I-expressing plasmid into SYM-I cells and then checked the IRF-3-dependent IFN-β promoter activities after infection with Ni, Ni-CE, and CE(NiN) strains (Fig. 8A). Overexpression of wild-type RIG-I significantly enhanced IRF-3-dependent IFN-β promoter activity in Ni-CE-infected cells. However, we found that the overexpression did not enhance IFN-β promoter activities in Ni- and CE(NiN)-infected cells. This result indicated that Ni and CE(NiN) strains, but not Ni-CE strain, evade the activation of the RIG-I-mediated IRF-3 pathway.

Next, we investigated the effect of expression of a CARD-deleted mutant RIG-I (RIG-IC), which acts as a dominant-negative mutant of RIG-I (43), on IRF-3-dependent IFN-β promoter activity in Ni-, Ni-CE-, or CE(NiN)-infected cells (Fig. 8B). Expression of RIG-IC significantly reduced IRF-3-dependent IFN-β promoter activity induced by infection of Ni-CE strain. On the other hand, RIG-IC did not change the IFN-β promoter activity induced by CE(NiN) strain. Furthermore, we found that IRF-3-dependent IFN-β promoter activity of Ni-CE-infected cells, but not that of CE(NiN)-infected cells, was reduced dose dependently by expression of RIG-IC (Fig. 8C). These findings indicated that the Ni and CE(NiN) strains, but not Ni-CE strain, evade the activation of RIG-I. To further confirm where the evasion of the RIG-I-mediated IRF-3 pathway occurs, we used a carboxy terminally truncated RIG-I (RIG-IN), which is a constitutively active mutant (43). We measured IRF-3-dependent IFN-β promoter activities in RIG-IN-transfected SYM-I cells after each virus infection (Fig. 8D). Expression of RIG-IN induced IRF-3-dependent IFN-β promoter activity without virus infection as expected. Importantly, expression of RIG-IN enhanced the IFN-β promoter activity equivalently in Ni-, Ni-CE-, and CE(NiN)-infected cells. Similar results were obtained by using an expression plasmid of IPS-1, which is an adopter molecule of RIG-I, to activate the

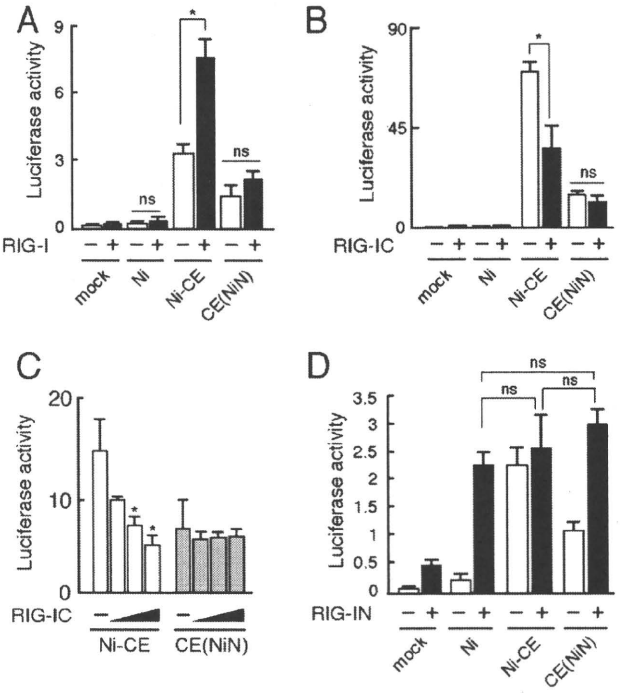

FIG. 8. Ni N protein, but not Ni-CE N protein, functions to evade activation of RIG-I-mediated antiviral response. (A) SYM-I cells were cotransfected with pRL-TK, 4×IRF-3-Luc, and 1 μg of pEF-Flag-RIG-I or empty vector. At 24 h posttransfection, the cells were infected with Ni, Ni-CE, and CE(NiN) strains at an MOI of 2 and incubated for 24 h. Then, the cells were lysed and luciferase activities were measured. *, Significant difference ($P < 0.01$); ns, no significant difference. (B) SYM-I cells were inoculated, in suspension, with each virus strain at an MOI of 2 FFU/cells and seeded. After 24 h, cells were transfected with pRL-TK, 4×IRF-3-Luc, and 1 μg of pEF-Flag-RIG-IC. After 24 h, the cells were lysed and luciferase activities were measured. *, Significant difference ($P < 0.01$); ns, no significant difference. (C) SYM-I cells were inoculated, in suspension, with each virus strain at an MOI of 2 FFU/cells and seeded. After 24 h, cells were transfected with pRL-TK, 4×IRF-3-Luc, and 0.5, 1, or 2 μg of pEF-Flag-RIG-IC. After 24 h, the cells were lysed, and the luciferase activities were measured. *, Significant difference versus mock-transfected cells ($P < 0.01$). (D) SYM-I cells were inoculated, in suspension, with each virus strain at an MOI of 2 FFU/cells and seeded. After 24 h, cells were transfected with pRL-TK, 4×IRF-3-Luc, and 1 μg of pEF-Flag-RIG-IN. After 24 h, the cells were lysed, and the luciferase activities were measured. The data are presented as means (± the SD) of three independent replicates. ns, No significant difference.

IRF-3 pathway (data not shown). These results indicated that Ni and CE(NiN) strains do not inhibit the IRF-3-dependent IFN-β promoter activity induced by activated RIG-I. Taken together, the results showed that Ni N protein, but not Ni-CE N protein, functions to inhibit activation of RIG-I.

We then hypothesized that CE(NiN) strain, but not Ni-CE strain, can evade antiviral responses ascribed to activation of RIG-I. To confirm this, we examined the ability of Ni-CE and CE(NiN) strains to replicate in RIG-I- or RIG-IN-expressing cells. RIG-I- or RIG-IN-expressing 293T cells were infected with Ni-CE- or CE(NiN) strain, and expression levels of their N proteins were compared by Western blotting, followed by quantification using a densitometer. As the expression levels of RIG-I increased, expression level of N protein of Ni-CE strain,

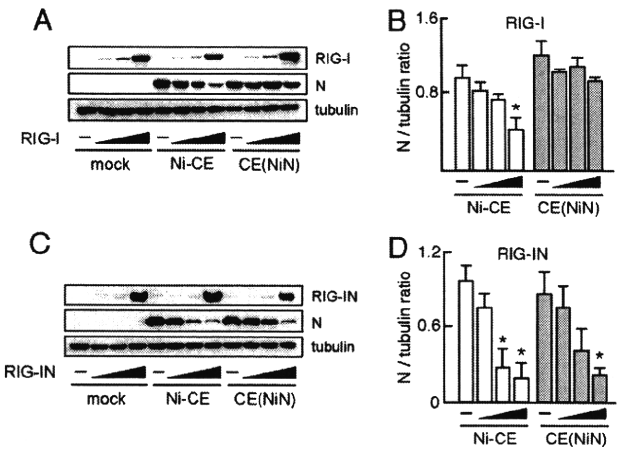

FIG. 9. CE(NiN) strain efficiently replicates in cells overexpressing RIG-I, but not RIG-IN. 293T cells were transfected with 0.05, 0.1, and 1 μg of pEF-Flag-RIG-I (A) or pEF-Flag-RIG-IN (C). After 24 h, cells were infected with Ni-CE and CE(NiN) strains at an MOI of 3. At 24 hpi, the cells were lysed and N protein, tubulin, RIG-I and RIG-IN were detected by Western blotting. (B and D) Ratio of each N protein band to its tubulin control was calculated by using ImageJ. Panels B and D show the results of experiments using pEF-Flag-RIG-I (A) and pEF-Flag-RIG-IN (C), respectively. Each bar represents the mean (± the SD) of three independent replicates. *, Significant difference versus mock-transfected cells ($P < 0.01$).

but not that of CE(NiN) strain, was decreased significantly (Fig. 9A and B). On the other hand, the expression levels of N protein of both strains were decreased by RIG-IN in a dose-dependent fashion (Fig. 9C and D). Taken together, these results indicate that Ni N, but not Ni-CE N, functions to evade activation of RIG-I and, subsequently, the induced antiviral responses.

DISCUSSION

A DNA microarray is a strong tool for comprehensive analysis of cellular gene expression and has been widely used in many research fields, including molecular biology and medicine. It has also been used to examine the effects of rabies virus infection on host gene expression (32, 41). For example, Wang et al. (41) reported that expression levels of innate immunity-related genes, including *IFN*-β, *CXCL10*, and *CCL5*, in the mouse brain infected with a street rabies virus (a field isolate from a silver-haired bat) are lower than the levels in the mouse brain infected with a less-virulent fixed rabies virus. This strongly suggests that evasion of innate immunity is important for high pathogenicity of rabies virus. However, the viral gene that is related to this phenomenon has not been identified yet, mainly due to the great genetic difference between street and fixed rabies viruses. In the present study, we comprehensively compared effects of infection with avirulent Ni-CE and virulent CE(NiN) strains on host gene expressions using a DNA microarray. Since these two strains are genetically identical except for the N gene, we thought that the differences between gene expressions in Ni-CE- and CE(NiN)-infected cells would give us an insight into N gene function, which is related to the different pathogenicities of the strains. We found that Ni-CE infection induces several innate immunity-related and inflammatory genes (e.g., *IFN*-β, *CCL5*, *CXCL10*, and *CXCL11*) more efficiently than does CE(NiN) infection. This finding clearly indicated that the N gene of rabies virus (virulent Ni strain) functions to evade host innate immunity and inflammation.

We previously reported that Ni and CE(NiN) strains, but not Ni-CE strain, kill adult mice after i.c. inoculation (35). We found that Ni and CE(NiN) strains grow more efficiently in the mouse brain than does Ni-CE strain: titers of Ni and CE(NiN) strains reached 10^8 and 10^4 FFU/g, respectively, whereas the titer of Ni-CE strain was less than 10^2 FFU/g at 3 days after i.c. inoculation with 100 FFU of each virus (K. Shimizu, unpublished data). This strongly suggests that host innate immunity is involved in the different growth rates of the strains in the mouse brain at the early stage of infection. Therefore, we considered that evasion of antiviral response by Ni N protein determines the viral pathogenicity in adult mice.

Some studies have shown that N protein of measles virus, which belongs to the family *Paramyxoviridae*, participates in systemic immunosuppression: measles virus N protein binds to the Fc receptor on B cells and dendritic cells and consequently induces immunosuppression by inhibiting antibody production (34) and impairing dendritic cell function (25), respectively. These studies indicated that the measles virus N protein plays an important role in evasion of host acquired immunity. Furthermore, it has been suggested that nucleoprotein of Ebola virus plays a role in the evasion of the IFN-induced antiviral response (10). On the other hand, to our knowledge, the present study is the first study showing that the *Mononegavirales* N protein functions to evade induction of host IFN and chemokines.

In the present study, we showed that Ni N protein, but not Ni-CE N protein, functions to evade activation of the IRF-3 pathway in the presence of other viral components (Fig. 6). We previously reported that there are only three amino acid changes between the two N proteins (Phe to Leu at position 273 [indicated as a mutation from Ni strain to Ni-CE strain], Tyr to His at position 394, and Phe to Leu at position 395) (35). These mutations may change the structure of N protein and possibly affect its interaction with other viral components. It is known that N protein physically interacts with P protein and viral genomic RNA (3). Notably, a previous study indicated that rabies virus P protein functions to block the IRF-3 pathway (6). Therefore, we hypothesized that Ni N protein increases inhibitory activity of P protein on the IRF-3 pathway or the expression level. However, our data indicated that Ni N protein did not affect this activity and the expression level of P protein of each virus (Fig. 7).

Our data indicated that N protein of Ni strain functions to evade activation of RIG-I (Fig. 8 and 9). Some studies have suggested that single-stranded RNA with a 5′-triphosphate end, such as virus genomic RNA of rabies virus, activates RIG-I (16, 31). It has also been reported that nonencapsidated genomic RNA of rabies virus is recognized by RIG-I and then induces the production of type I IFN (16). Recently, Albertini et al. (4) determined the crystal structure of rabies virus N protein and showed that the N protein is composed of two domains, an N-terminal domain (NTD; amino acid residues 32 to 233) and a C-terminal domain (CTD; residues 236 to 356 and 396 to 450). It was also shown that the NTD and CTD

clamp down onto the RNA strand (viral genomic RNA homolog) and enclose it completely. Based on these findings, these authors pointed out the possibility that the closed form of the N-RNA complex protects the viral genome from recognition by cellular RIG-I or Toll-like receptors, which are known to be viral RNA sensors and to play important roles in host innate immunity (3, 4). Therefore, we hypothesized that the three amino acid changes between Ni and Ni-CE N proteins, which are all located in the CTD, would affect the N-RNA interaction and, consequently, the structure of the RNP complex. It would be interesting to determine whether or not the genomic RNA encapsidated by the Ni-CE N protein is recognized more efficiently by RIG-I than the RNA with Ni N protein.

Encapsidation of genomic RNA by N protein of rabies virus plays vital roles in regulation of viral RNA replication (3). Therefore, it is also possible that Ni N protein, but not Ni-CE N protein, limits the replication efficiency of the viral genomic RNA and consequently suppresses the activation of RIG-I. However, our data indicated that the amounts of viral genomic and antigenomic RNAs in Ni-CE-infected SYM-I cells at 6, 12, and 24 hpi were comparable to those in CE(NiN)-infected cells (Fig. 1B). Therefore, we concluded that there is no clear difference between genome replications of Ni-CE strain and CE(NiN) strain. On the other hand, it has recently been shown that RIG-I is activated by short double-stranded RNA (19) and short-hairpin RNA (22). Thus, the exact structure of RNA activating RIG-I remains controversial. We are just starting to search for an actual ligand of RIG-I produced in Ni-CE-infected cells.

Although both Ni and CE(NiN) strains cause lethal infection in adult mice after i.c. inoculation, the Ni strain is much more virulent than the CE(NiN) strain: only 10 FFU of Ni strain is sufficient to kill 100% of adult mice by i.c. inoculation, whereas 1,000 FFU of CE(NiN) strain is required to do so (35). In the present study, we showed that expression levels of many host genes, including IFN-β and chemokine genes, in Ni-infected cells are much lower than those in CE(NiN)-infected cells (Fig. 2 and 3). These low expression levels of genes are attributed to low growth rate and the replication efficiency of viral genomic and antigenomic RNAs of Ni strain (Fig. 1B). In addition, we previously reported that not only the N gene but also the P and M genes are related to the difference between pathogenicities of Ni and Ni-CE strains (35). We also showed that Ni P and M genes are involved in the low sensitivity to type I IFN (36) and low cytopathogenicity (28), respectively. Therefore, P and M genes, together with the N gene, might be important for suppression of the expression of host defense-related genes.

The present study has revealed a novel function of rabies virus N protein by showing that the protein functions to evade activation of RIG-I and inhibit activation of the IRF-3 pathway. To our knowledge, this is the first report that the *Mononegavirales* N protein functions to evade induction of host IFN and chemokines. Further studies are needed to completely elucidate the molecular mechanism. We believe that our findings provide basic information for understanding the pathogenicity of rabies virus and also for identifying new targets for antiviral therapies.

ACKNOWLEDGMENTS

We thank A. Kawai (Research Institute for Production and Development, Kyoto, Japan) for providing SYM-I cells and anti-P polyclonal antibody. We also thank H. Fukushi and K. Ohya (Gifu University, Gifu, Japan) for providing the NDV B-1 strain. We are grateful to Y. Kawaoka (University of Tokyo), S. Ludwig (Westfaelische-Wilhelms University, Muenster, Germany), C. F. Basler (Mount Sinai School of Medicine, New York, NY), and T. Fujita (Kyoto University, Kyoto, Japan) for providing plasmids. We thank W. Kamitani (Osaka University, Osaka, Japan) for technical advice for the IRF-3 dimerization assay.

This study was partially supported by a grant (project code I-AD14-2009-11-01) from the National Veterinary Research and Quarantine Service, Ministry for Food, Agriculture, Forestry, and Fisheries (Korea) in 2008.

REFERENCES

1. **Akira, S., S. Uematsu, and O. Takeuchi.** 2006. Pathogen recognition and innate immunity. Cell **124**:783–801.
2. **Albertini, A. A., C. R. Clapier, A. K. Wernimont, G. Schoehn, W. Weissenhorn, and R. W. Ruigrok.** 2007. Isolation and crystallization of a unique size category of recombinant rabies virus nucleoprotein-RNA rings. J. Struct. Biol. **158**:129–133.
3. **Albertini, A. A., G. Schoehn, W. Weissenhorn, and R. W. Ruigrok.** 2008. Structural aspects of rabies virus replication. Cell Mol. Life Sci. **65**:282–294.
4. **Albertini, A. A., A. K. Wernimont, T. Muziol, R. B. Ravelli, C. R. Clapier, G. Schoehn, W. Weissenhorn, and R. W. Ruigrok.** 2006. Crystal structure of the rabies virus nucleoprotein-RNA complex. Science **313**:360–363.
5. **Basler, C. F., A. Mikulasova, L. Martinez-Sobrido, J. Paragas, E. Muhlberger, M. Bray, H. D. Klenk, P. Palese, and A. Garcia-Sastre.** 2003. The Ebola virus VP35 protein inhibits activation of interferon regulatory factor 3. J. Virol. **77**:7945–7956.
6. **Brzozka, K., S. Finke, and K. K. Conzelmann.** 2005. Identification of the rabies virus alpha/beta interferon antagonist: phosphoprotein P interferes with phosphorylation of interferon regulatory factor 3. J. Virol. **79**:7673–7681.
7. **Brzozka, K., S. Finke, and K. K. Conzelmann.** 2006. Inhibition of interferon signaling by rabies virus phosphoprotein P: activation-dependent binding of STAT1 and STAT2. J. Virol. **80**:2675–2683.
8. **Daffis, S., M. A. Samuel, B. C. Keller, M. Gale, Jr., and M. S. Diamond.** 2007. Cell-specific IRF-3 responses protect against West Nile virus infection by interferon-dependent and -independent mechanisms. PLoS Pathog. **3**:e106.
9. **Delhaye, S., S. Paul, G. Blakqori, M. Minet, F. Weber, P. Staeheli, and T. Michiels.** 2006. Neurons produce type I interferon during viral encephalitis. Proc. Natl. Acad. Sci. U. S. A. **103**:7835–7840.
10. **Ebihara, H., A. Takada, D. Kobasa, S. Jones, G. Neumann, S. Theriault, M. Bray, H. Feldmann, and Y. Kawaoka.** 2006. Molecular determinants of Ebola virus virulence in mice. PLoS Pathog. **2**:e73.
11. **Ehrhardt, C., C. Kardinal, W. J. Wurzer, T. Wolff, C. von Eichel-Streiber, S. Pleschka, O. Planz, and S. Ludwig.** 2004. Rac1 and PAK1 are upstream of IKK-epsilon and TBK-1 in the viral activation of interferon regulatory factor-3. FEBS Lett. **567**:230–238.
12. **Finke, S., and K. K. Conzelmann.** 2005. Replication strategies of rabies virus. Virus Res. **111**:120–131.
13. **Genin, P., M. Algarte, P. Roof, R. Lin, and J. Hiscott.** 2000. Regulation of RANTES chemokine gene expression requires cooperativity between NF-κB and IFN-regulatory factor transcription factors. J. Immunol. **164**:5352–5361.
14. **Honda, K., and T. Taniguchi.** 2006. IRFs: master regulators of signaling by Toll-like receptors and cytosolic pattern-recognition receptors. Nat. Rev. Immunol. **6**:644–658.
15. **Honda, Y., A. Kawai, and S. Matsumoto.** 1984. Comparative studies of rabies and Sindbis virus replication in human neuroblastoma (SYM-I) cells that can produce interferon. J. Gen. Virol. **65**(Pt. 10):1645–1653.
16. **Hornung, V., J. Ellegast, S. Kim, K. Brzozka, A. Jung, H. Kato, H. Poeck, S. Akira, K. K. Conzelmann, M. Schlee, S. Endres, and G. Hartmann.** 2006. 5′-Triphosphate RNA is the ligand for RIG-I. Science **314**:994–997.
17. **Ishikawa, Y., T. Samejima, T. Nunoya, T. Motohashi, and Y. Nomura.** 1989. Biological properties of the cell culture-adapted RC-HL strain of rabies virus as a candidate strain for an inactivated vaccine. J. Jpn. Vet. Med. Assoc. **42**:637–643.
18. **Kato, H., S. Sato, M. Yoneyama, M. Yamamoto, S. Uematsu, K. Matsui, T. Tsujimura, K. Takeda, T. Fujita, O. Takeuchi, and S. Akira.** 2005. Cell type-specific involvement of RIG-I in antiviral response. Immunity **23**:19–28.
19. **Kato, H., O. Takeuchi, E. Mikamo-Satoh, R. Hirai, T. Kawai, K. Matsushita, A. Hiiragi, T. S. Dermody, T. Fujita, and S. Akira.** 2008. Length-dependent recognition of double-stranded ribonucleic acids by retinoic acid-inducible gene-I and melanoma differentiation-associated gene 5. J. Exp. Med. **205**:1601–1610.
20. **Katze, M. G., J. L. Fornek, R. E. Palermo, K. A. Walters, and M. J. Korth.**

2008. Innate immune modulation by RNA viruses: emerging insights from functional genomics. Nat. Rev. Immunol. **8**:644–654.
21. **Kawai, T., K. Takahashi, S. Sato, C. Coban, H. Kumar, H. Kato, K. J. Ishii, O. Takeuchi, and S. Akira.** 2005. IPS-1, an adaptor triggering RIG-I- and Mda5-mediated type I interferon induction. Nat. Immunol. **6**:981–988.
22. **Kenworthy, R., D. Lambert, F. Yang, N. Wang, Z. Chen, H. Zhu, F. Zhu, C. Liu, K. Li, and H. Tang.** 2009. Short-hairpin RNAs delivered by lentiviral vector transduction trigger RIG-I-mediated IFN activation. Nucleic Acids Res. **37**:6587–6599.
23. **Lefort, S., A. Soucy-Faulkner, N. Grandvaux, and L. Flamand.** 2007. Binding of Kaposi's sarcoma-associated herpesvirus K-bZIP to interferon-responsive factor 3 elements modulates antiviral gene expression. J. Virol. **81**:10950–10960.
24. **Loo, Y. M., D. M. Owen, K. Li, A. K. Erickson, C. L. Johnson, P. M. Fish, D. S. Carney, T. Wang, H. Ishida, M. Yoneyama, T. Fujita, T. Saito, W. M. Lee, C. H. Hagedorn, D. T. Lau, S. A. Weinman, S. M. Lemon, and M. Gale, Jr.** 2006. Viral and therapeutic control of IFN-beta promoter stimulator 1 during hepatitis C virus infection. Proc. Natl. Acad. Sci. U. S. A. **103**:6001–6006.
25. **Marie, J. C., J. Kehren, M. C. Trescol-Biemont, A. Evlashev, H. Valentin, T. Walzer, R. Tedone, B. Loveland, J. F. Nicolas, C. Rabourdin-Combe, and B. Horvat.** 2001. Mechanism of measles virus-induced suppression of inflammatory immune responses. Immunity **14**:69–79.
26. **Mavrakis, M., F. Iseni, C. Mazza, G. Schoehn, C. Ebel, M. Gentzel, T. Franz, and R. W. Ruigrok.** 2003. Isolation and characterization of the rabies virus N degrees-P complex produced in insect cells. Virology **305**:406–414.
27. **Minamoto, N., H. Tanaka, M. Hishida, H. Goto, H. Ito, S. Naruse, K. Yamamoto, M. Sugiyama, T. Kinjo, K. Mannen, and K. Mifune.** 1994. Linear and conformation-dependent antigenic sites on the nucleoprotein of rabies virus. Microbiol. Immunol. **38**:449–455.
28. **Mita, T., K. Shimizu, N. Ito, K. Yamada, Y. Ito, M. Sugiyama, and N. Minamoto.** 2008. Amino acid at position 95 of the matrix protein is a cytopathic determinant of rabies virus. Virus Res. **137**:33–39.
29. **Nakaya, T., M. Sato, N. Hata, M. Asagiri, H. Suemori, S. Noguchi, N. Tanaka, and T. Taniguchi.** 2001. Gene induction pathways mediated by distinct IRFs during viral infection. Biochem. Biophys. Res. Commun. **283**:1150–1156.
30. **Onoguchi, K., M. Yoneyama, A. Takemura, S. Akira, T. Taniguchi, H. Namiki, and T. Fujita.** 2007. Viral infections activate types I and III interferon genes through a common mechanism. J. Biol. Chem. **282**:7576–7581.
31. **Pichlmair, A., O. Schulz, C. P. Tan, T. I. Naslund, P. Liljestrom, F. Weber, and C. Reis e Sousa.** 2006. RIG-I-mediated antiviral responses to single-stranded RNA bearing 5′-phosphates. Science **314**:997–1001.
32. **Prehaud, C., F. Megret, M. Lafage, and M. Lafon.** 2005. Virus infection switches TLR-3-positive human neurons to become strong producers of beta interferon. J. Virol. **79**:12893–12904.
33. **Randall, R. E., and S. Goodbourn.** 2008. Interferons and viruses: an interplay between induction, signaling, antiviral responses and virus countermeasures. J. Gen. Virol. **89**:1–47.
34. **Ravanel, K., C. Castelle, T. Defrance, T. F. Wild, D. Charron, V. Lotteau, and C. Rabourdin-Combe.** 1997. Measles virus nucleocapsid protein binds to FcγRII and inhibits human B-cell antibody production. J. Exp. Med. **186**:269–278.
35. **Shimizu, K., N. Ito, T. Mita, K. Yamada, J. Hosokawa-Muto, M. Sugiyama, and N. Minamoto.** 2007. Involvement of nucleoprotein, phosphoprotein, and matrix protein genes of rabies virus in virulence for adult mice. Virus Res. **123**:154–160.
36. **Shimizu, K., N. Ito, M. Sugiyama, and N. Minamoto.** 2006. Sensitivity of rabies virus to type I interferon is determined by the phosphoprotein gene. Microbiol. Immunol. **50**:975–978.
37. **Takahasi, K., M. Yoneyama, T. Nishihori, R. Hirai, H. Kumeta, R. Narita, M. Gale, Jr., F. Inagaki, and T. Fujita.** 2008. Nonself RNA-sensing mechanism of RIG-I helicase and activation of antiviral immune responses. Mol. Cell **29**:428–440.
38. **Vidy, A., M. Chelbi-Alix, and D. Blondel.** 2005. Rabies virus P protein interacts with STAT1 and inhibits interferon signal transduction pathways. J. Virol. **79**:14411–14420.
39. **Vidy, A., J. El Bougrini, M. K. Chelbi-Alix, and D. Blondel.** 2007. The nucleocytoplasmic rabies virus P protein counteracts interferon signaling by inhibiting both nuclear accumulation and DNA binding of STAT1. J. Virol. **81**:4255–4263.
40. **Wagoner, J., M. Austin, J. Green, T. Imaizumi, A. Casola, A. Brasier, K. S. Khabar, T. Wakita, M. Gale, Jr., and S. J. Polyak.** 2007. Regulation of CXCL-8 (interleukin-8) induction by double-stranded RNA signaling pathways during hepatitis C virus infection. J. Virol. **81**:309–318.
41. **Wang, Z. W., L. Sarmento, Y. Wang, X. Q. Li, V. Dhingra, T. Tseggai, B. Jiang, and Z. F. Fu.** 2005. Attenuated rabies virus activates, while pathogenic rabies virus evades, the host innate immune responses in the central nervous system. J. Virol. **79**:12554–12565.
42. **Yamada, K., N. Ito, M. Takayama-Ito, M. Sugiyama, and N. Minamoto.** 2006. Multigenic relation to the attenuation of rabies virus. Microbiol. Immunol. **50**:25–32.
43. **Yoneyama, M., M. Kikuchi, T. Natsukawa, N. Shinobu, T. Imaizumi, M. Miyagishi, K. Taira, S. Akira, and T. Fujita.** 2004. The RNA helicase RIG-I has an essential function in double-stranded RNA-induced innate antiviral responses. Nat. Immunol. **5**:730–737.

JOURNAL OF VIROLOGY, July 2010, p. 6699–6710 Vol. 84, No. 13
0022-538X/10/$12.00 doi:10.1128/JVI.00011-10

Role of Interferon Antagonist Activity of Rabies Virus Phosphoprotein in Viral Pathogenicity▽

Naoto Ito,[1,2]§* Gregory W. Moseley,[3]§ Danielle Blondel,[4] Kenta Shimizu,[2] Caitlin L. Rowe,[3] Yuki Ito,[2] Tatsunori Masatani,[2] Keisuke Nakagawa,[2] David A. Jans,[3] and Makoto Sugiyama[1,2]

Laboratory of Zoonotic Diseases, Faculty of Applied Biological Sciences,[1] and the United Graduate School of Veterinary Sciences,[2] Gifu University, 1-1 Yanagido, Gifu 501-1193, Japan; Nuclear Signalling Laboratory, Department of Biochemistry and Molecular Biology, Monash University, Monash, Victoria 3800, Australia[3]; and Unité de Virologie Moléculaire et Structurale UPR 3296, 91198 Gif sur Yvette Cedex, France[4]

Received 5 January 2010/Accepted 21 April 2010

The fixed rabies virus (RV) strain Nishigahara kills adult mice after intracerebral inoculation, whereas the chicken embryo fibroblast cell-adapted strain Ni-CE causes nonlethal infection in adult mice. We previously reported that the chimeric CE(NiP) strain, which has the phosphoprotein (P protein) gene from the Nishigahara strain in the genetic background of the Ni-CE strain, causes lethal infection in adult mice, indicating that the P gene is responsible for the different pathogenicities of the Nishigahara and Ni-CE strains. Previous studies demonstrated that RV P protein binds to the interferon (IFN)-activated transcription factor STAT1 and blocks IFN signaling by preventing its translocation to the nucleus. In this study, we examine the molecular mechanism by which RV P protein determines viral pathogenicity by comparing the IFN antagonist activities of the Nishigahara and Ni-CE P proteins. The results, obtained from both RV-infected cells and cells transfected to express P protein only, show that Ni-CE P protein is significantly impaired for its capacity to block IFN-activated STAT1 nuclear translocation and, consequently, inhibits IFN signaling less efficiently than Nishigahara P protein. Further, it was demonstrated that a defect in the nuclear export of Ni-CE P protein correlates with a defect in its ability to cause the mislocalization of STAT1. These data provide the first evidence that the capacity of the RV P protein to inhibit STAT1 nuclear translocation and IFN signaling correlates with the viral pathogenicity.

The host immune response to viral infection is a key factor in defining viral pathogenicity and the outcome of the infection. This depends not only on the capacity of the host to mount an innate and/or adaptive immune response against the virus but also on the ability of the virus to evade/subvert this response (22).

The principal response of host cells to viral infection is the production of type I interferons (IFNs) (including alpha interferon [IFN-α] and IFN-β), which, on binding to IFN receptors on the cell surface, activate the JAK/STAT intracellular signaling pathway that culminates in the phosphorylation, heterodimerization, and nuclear translocation of the transcription factors *s*ignal *t*ransducer and *a*ctivator of *t*ranscription 1 (STAT1) and STAT2. In the context of a complex called IFN-stimulated gene factor 3 (ISGF3), the activated STATs bind to promoters in the DNA that contain an IFN-stimulated response element (ISRE) sequence, resulting in the transcription of a plethora of IFN-stimulated genes (ISGs) encoding antiviral proteins which act to establish the antiviral state in cells (reviewed in reference 22).

To propagate efficiently in host cells, viruses have had to evolve multiple strategies to dampen the host IFN system, which appear to involve the expression of viral proteins with IFN antagonist functions. These IFN antagonists are reported to exert their effect by a variety of mechanisms, reflecting the diversity of host antiviral responses, but the STATs are known as common targets of viral IFN antagonists, presumably because of their pivotal role in IFN signaling. For example, nonsegmented negative-strand RNA viruses (order *Mononegavirales*, which is composed of four families, *Paramyxoviridae*, *Rhabdoviridae*, *Filoviridae*, and *Bornaviridae*) are known to express proteins that act as IFN antagonists by targeting STATs. These include the VP24 protein of Ebola virus (24), belonging to the family *Filoviridae*, and the V protein of Nipah virus (25), a member of the family *Paramyxoviridae*, which are reported to prevent STAT nuclear accumulation. Similarly, the phosphoprotein (P protein) of rabies virus (RV), a prototype of the family *Rhabdoviridae*, has been identified as its viral IFN antagonist and has the capacity to block multiple stages of STAT1-dependent IFN signaling. Namely, RV P protein binds to STAT1 and inhibits not only the nuclear import of IFN-activated STAT1 (4, 17, 36) but also the binding of ISGF3 to DNA containing the ISRE sequence (37). Furthermore, it was reported that RV P protein binds to STAT2 and inhibits its nuclear translocation induced by IFN-α (4).

During infection, RV efficiently replicates in neurons and causes lethal encephalomyelitis. As neurons are able to produce type I IFN in response to viral infection and are responsive to type I IFN (6), it appears that circumventing the host IFN system would be a key factor for pathogenicity of RV. However, there is little data to link the IFN antagonism by RV P protein with viral pathogenicity directly. We previously reported that the RV strain Nishigahara kills adult mice after

* Corresponding author. Mailing address: Laboratory of Zoonotic Diseases, Faculty of Applied Biological Sciences, Gifu University, 1-1 Yanagido, Gifu 501-1193, Japan. Phone and fax: 81 58 293 2949. E-mail: address: naotoito@gifu-u.ac.jp.

§ N.I. and G.W.M. contributed equally to this study.

▽ Published ahead of print on 28 April 2010.

intracerebral (i.c.) inoculation, whereas the Ni-CE strain, which we have established after 100 passages of Nishigahara strain in chicken embryo fibroblast cells, causes nonlethal infection in adult mice (30). Using a reverse genetics approach, we found that the chimeric virus strain CE(NiP), which has the P protein-encoding P gene from the Nishigahara strain in the genetic background of the Ni-CE strain, kills adult mice after i.c. inoculation (30). We recently demonstrated that a key difference between the virulent Nishigahara and CE(NiP) strains and the avirulent Ni-CE strain is their sensitivity to IFN-α: Nishigahara and CE(NiP) strains are more resistant to IFN-α than the Ni-CE strain (31). This finding led us to the hypothesis that the RV P protein is a key regulator of viral pathogenicity, dependent on its capacity to inhibit IFN signaling.

In the present study, we examine the molecular mechanisms underlying the role of P protein in RV pathogenicity by comparing the inhibitory effects of the Nishigahara and Ni-CE P proteins on type I IFN signaling. The results obtained from both RV-infected cells and transfected cells transiently expressing P protein demonstrate that the Ni-CE P protein is significantly impaired in its capacity to block IFN-activated STAT1 nuclear translocation and, consequently, inhibits IFN signaling less efficiently than does Nishigahara P protein. Further, we find that the nuclear export of Ni-CE P protein is defective and that this correlates with a defect in its ability to cause mislocalization of STAT1. This study provides the first evidence that RV P protein's ability to inhibit STAT1 nuclear translocation and IFN signaling correlates with the pathogenicity of RV.

MATERIALS AND METHODS

Cells and viruses. Human neuroblastoma SK-N-SH cells (ATCC number HTB-11) and mouse neuroblastoma NA cells were maintained in Eagle's minimal essential medium supplemented with 10% fetal calf serum. Vero cells were grown in Dulbecco's modified Eagle's medium with 10% fetal calf serum. For infection with the RV Nishigahara and Ni-CE strains, we used recombinant virus of the respective strain which had been recovered from cloned cDNA (30, 38). The chimeric CE(NiP) strain, which has the Nishigahara P protein gene (P gene) in the genetic background of strain Ni-CE, was previously generated by a reverse genetics system (Fig. 1A) (30). Stocks of these RV strains were prepared in NA cells.

Propagation of RV in mouse brains. Virus propagation in the mouse brain was examined as described previously (33, 34). Briefly, 6-week-old female ddY mice (Japan SLC, Inc., Japan) were inoculated intracerebrally with 100 focus forming units (FFU) of each strain. Two inoculated mice were euthanized daily, and then their brains were mixed and homogenized. The virus titer in the homogenates (calculated as FFU/g) was determined by a focus assay on confluent NA cells after 10-fold weight/volume dilution of the homogenates and collection of the supernatants. The viral foci were visualized by indirect fluorescent antibody staining with anti-RV N protein mouse monoclonal antibody 13-27 (14) after fixation of the cells with 2% paraformaldehyde for 30 min and 100% methanol for 2 min. This animal experiment was conducted in accordance with the Standards Relating to the Care and Management of Experimental Animals promulgated by Gifu University, Japan (allowance no. 08119).

IFN-α sensitivity of RV. SK-N-SH cells were inoculated with each virus at a multiplicity of infection (MOI) of 0.01 and then were cultured in growth medium with or without 500 U/ml of human IFN-α2a (PBL InterferonSource, Piscataway, NJ). At 3 days postinoculation (p.i.), the supernatant of the culture medium was collected and stored at −80°C until virus titration. The virus titer in the culture medium (calculated as FFU/ml) was determined by a focus assay on confluent NA cells as described above. Preliminary experiments showed that the concentration of IFN-α used in this experiment (500 U/ml) did not affect the accuracy of this virus titration (data not shown). The IFN sensitivity index of each strain

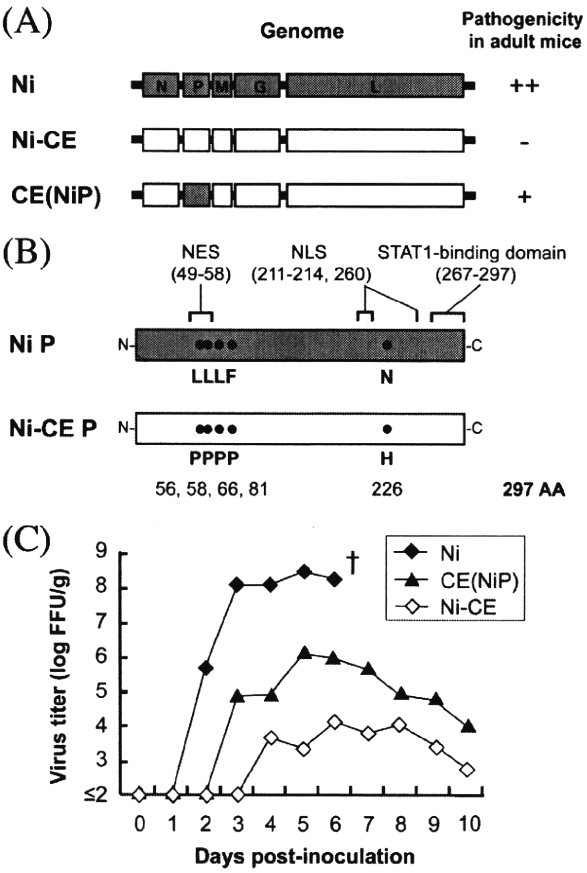

FIG. 1. Characteristics of the RV strains and P proteins used in this study. (A) Genome organization and pathogenicities of the Nishigahara (Ni), Ni-CE, and chimeric CE(NiP) strains. The pathogenicity of each strain for adult mice was previously determined by i.c. inoculation with 1,000 FFU of each virus (30). ++, lethal (all mice died within 7 days); +, lethal (all mice died within 14 days); −, not lethal (all mice survived). (B) Amino acid differences between Nishigahara and Ni-CE P proteins are highlighted. The previously identified nuclear export signal (NES), nuclear localization signal (NLS) (20), and STAT1-binding domain (36) are also indicated. AA, amino acids. (C) Propagation of Nishigahara, Ni-CE, and CE(NiP) strains in adult mouse brains. The virus titers in the mouse brains were determined as previously described (34). †, All Nishigahara-inoculated mice died after this time point.

was determined by the logarithm of the virus titer in SK-N-SH cells (untreated) minus that of the titer in SK-N-SH cells treated with IFN-α.

To examine virus propagation in terms of viral protein synthesis levels in the presence of IFN-α, the SK-N-SH cells were inoculated with each virus at an MOI of 0.01 and then were cultured in growth medium containing 0 to 500 U/ml IFN-α. At 2 days p.i., the cells were lysed in lysis buffer (20 mM Tris [pH 8.0], 150 mM NaCl, 2 mM EDTA, 20 mM CHAPS {3-[(3-cholamidopropyl)-dimethylammonior]-1-propanesulfonate}, 4 mM p-APMSF [(*p*-4-amidinophenyl)methanesulfonyl fluoride hydrochloride monohydrate]) and the solubilized protein was analyzed by Western blotting as described below.

Western blotting. Cell lysate samples were separated by sodium dodecyl sulfate (SDS)–10% polyacrylamide gel electrophoresis before transfer to a polyvinylidene difluoride (PVDF) membrane (Immobilon transfer membranes; Millipore, Billerica, MA). RV N and P proteins on the membrane were visualized by immunoblotting with anti-N protein monoclonal antibody 13-27 (14) and anti-P protein rabbit serum (kindly provided by Akihiko Kawai), respectively. Alpha-tubulin was also detected, as a loading control, by using anti-monoclonal anti-

tubulin antibody (Sigma, Saint Louis, MO). The intensities of the protein bands were quantified with Image J software (http://rsbweb.nih.gov/ij/).

Plasmid constructions. The Nishigahara P protein-expressing plasmid pcDNA-NiP, with cDNA corresponding to the Nishigahara P gene cloned into the pcDNA1.1/Amp vector (Invitrogen, Carlsbad, CA), has been described previously (38). The construct pcDNA-CEP, containing the cDNA for the Ni-CE P gene, was produced similarly. To express green fluorescent protein (GFP)-tagged P proteins of Nishigahara and Ni-CE strains (designated Ni P-GFP and Ni-CE P-GFP, respectively), we cloned the cDNA fragment of the P gene from the respective strain into the pEGFP-N1 vector (Clontech, Mountain View, CA). To express the Ni-CE P-GFP mutant with proline (Pro)-to-leucine (Leu) substitutions at positions 56 and 58 of the Ni-CE P protein [designated Ni-CE P(NES$^+$)-GFP], we mutated the pEGFP-N1 plasmid expressing Ni-CE P-GFP by using a QuikChange II site-directed mutagenesis kit (Stratagene, La Jolla, CA). For the yeast two-hybrid analysis described below, we cloned the cDNA fragment of the Nishigahara or Ni-CE P gene into the plasmid vector pLex10 (pLexA) (kindly provided by Jacques Camonis), which contains the yeast-selectable TRP1 gene and the LexA DNA-binding domain (BD) coding sequence, to express BD-fused Nishigahara and Ni-CE P proteins. The resulting plasmids were designated pLex-Ni P and pLex-Ni-CE P, respectively.

ISRE reporter assay. SK-N-SH cells grown in a 24-well tissue culture plate were transfected with 0.04 μg of pRL-TK (Promega, Madison, WI), which expresses the *Renilla* luciferase, and 0.25 μg of pISRE-Luc (Stratagene), which has an ISRE-containing promoter upstream of the firefly luciferase reporter gene, using Lipofectamine 2000 (Invitrogen). At 24 h after transfection, the cells were inoculated with the Nishigahara, Ni-CE, or CE(NiP) strain at an MOI of 3 and incubated for 6 h prior to treatment with or without 2,000 U/ml of IFN-α2a for 12 h. After lysis of the cells, the activities of firefly and *Renilla* luciferases were determined by using a dual-luciferase-reporter assay system (Promega, Madison, WI) according to the manufacturer's instructions. The ISRE activity was calculated as firefly luciferase activity normalized to *Renilla* luciferase activity.

In other experiments, SK-N-SH cells were transfected with 0.25 μg of pcDNA-NiP, pcDNA-CEP, or pcDNA-NiN expressing Nishigahara N protein (38) or an empty vector (pcDNA1.1/Amp), together with pRL-TK and pISRE-Luc. At 24 h after transfection, the cells were treated with or without 2,000 U/ml of IFN-α2a for 6 h and the activities of the firefly and *Renilla* luciferases were determined as described above. In some cases, pEGFP-N1 plasmids expressing Ni P-GFP, Ni-CE P-GFP, or Ni-CE P(NES$^+$)-GFP were employed instead of these pcDNA1.1/Amp plasmids, using the same experimental conditions described above.

Real-time reverse transcription (RT)-PCR. SK-N-SH cells grown in a 24-well tissue culture plate were inoculated with the Nishigahara, Ni-CE, or CE(NiP) strain at an MOI of 3 and incubated for 6 h prior to treatment with 2,000 U/ml of IFN-α2a for 12 h. The expression of myxovirus resistance A (*MxA*) and glyceraldehyde 3-phosphate dehydrogenase (*GAPDH*) genes in the infected cells was analyzed by using a TaqMan gene expression Cells-to-CT kit (Ambion, Austin, TX) with specific TaqMan probes (*MxA* [Hs00182073] and *GAPDH* [4326317E]; Applied Biosystems, Carlsbad, CA) in an ABI 7300 real-time PCR system (Applied Biosystems). The expression levels of the *MxA* gene are indicated as the number of copies of specific mRNA per copy of human *GAPDH* mRNA. All assays were carried out in triplicate, and the results are expressed as means ± standard deviations.

Immunostaining. SK-N-SH cells grown in an 8-chamber culture slide (BD Falcon; BD Biosciences, Franklin Lakes, NJ) were inoculated with each strain at an MOI of 0.01 and then were treated with or without IFN-α (4,000 U/ml) for 30 min at 24 h p.i. The cells were fixed with 3.7% formaldehyde for 10 min and 90% methanol for 5 min and immunostained with an anti-STAT1 rabbit antibody (sc-346; Santa Cruz Biotechnology, Santa Cruz, CA) and an anti-RV N protein mouse monoclonal antibody, followed by incubation with Alexa Fluor 488 anti-rabbit IgG (Invitrogen) (green) and Alexa Fluor 594 anti-mouse IgG (Invitrogen) (red). The stained samples were analyzed by confocal laser scanning microscopy (CLSM), using a Leica SP5 microscope with 63× glycerol immersion objective. In some experiments, RV P protein in infected SK-N-SH cells was immunostained by using anti-P protein rabbit serum and Alexa Fluor 488 anti-rabbit IgG.

Subcellular localization of GFP-tagged P protein and STAT1 protein. Vero cells or SK-N-SH cells were grown on coverslips and transfected with the pEGFP-N1 plasmid expressing Ni P-GFP, Ni-CE P-GFP, or Ni-CE P(NES$^+$)-GFP by using Lipofectamine 2000 as previously described (18, 26). For costaining of cells for STAT1, cells were treated with or without IFN-α for 1 h before fixation and permeabilization as described above. Cells were immunostained with anti-STAT1 (610185; BD Biosciences) followed by Alexa 568-coupled secondary antibody (Invitrogen) and imaged using a Leica SP5 microscope as described above.

Yeast two-hybrid analysis. Yeast cells (L40 strain) containing His3- and LacZ-responsive reporter genes were transformed with pLex-Ni P or -Ni-CE P, together with the plasmid pGAD-STAT1 (36), which has the yeast-selectable LEU2 gene and expresses the GAL4 activation domain (AD)-fused STAT1. A combination of pLex-P CVS expressing BD-fused P protein from the RV CVS strain (36) and pGAD-STAT1 was also used as a positive control. The RV P protein-STAT1 interaction was assayed by the expression of the His3 reporter gene on a plate lacking the amino acids tryptophan (Trp), Leu, and histidine (His) and also by the appearance of blue colonies following X-Gal (5-bromo-4-chloro-3-indolyl-β-D-galactosidase) overlay as follows: an X-Gal mixture containing 0.5% agar, 0.1% SDS, 6% dimethylformamide, and 0.04% X-Gal was overlaid on fresh transformants grown on a plate lacking Trp and Leu. Blue colonies were detected after 60 min to 18 h at 30°C.

Coimmunoprecipitation (co-IP). SK-N-SH cells in a 60-mm tissue culture dish were infected with the Ni-CE or CE(NiP) strain at an MOI of 0.1 and incubated for 18 h prior to treatment with 2,000 U/ml of IFN-α2a for 2 h. After the cells were washed once with ice-cold phosphate-buffered saline (PBS), the cell lysates were prepared in radioimmunoprecipitation assay (RIPA) buffer (1% NP-40, 0.1% SDS, and 0.5% sodium deoxycholate in PBS) containing protease inhibitor cocktail (Complete mini; Roche, Germany) on ice for 20 min and centrifuged at 13,200 × *g* for 10 min at 4°C to remove cell debris. Supernatants were collected and precleared by incubation with 20 μl of Protein A/G Plus-Agarose immunoprecipitation reagent (Santa Cruz Biotechnology) and 2 μg of IgG from rabbit serum (Sigma) at 4°C for 45 min. After centrifugation at 800 × *g* for 1 min at 4°C, supernatants were incubated with 4 μg of anti-STAT1 rabbit antibody (sc-346; Santa Cruz Biotechnology) or rabbit IgG (control IgG) at 4°C for 2 h. The samples were incubated further with 20 μl of Protein A/G Plus-Agarose immunoprecipitation reagent at 4°C for 15 h. After centrifugation at 800 × *g* for 1 min at 4°C, the precipitated immune complexes were washed four times with RIPA buffer. Finally, the precipitated proteins were dissolved in sample buffer solution (2× 2-mercaptoethanol-added) (Wako Pure Chemical Industries, Japan) and analyzed by Western blotting using an anti-STAT1 rabbit antibody (sc-346; Santa Cruz Biotechnology) or anti-P protein rabbit serum as the primary antibody, with rabbit IgG TrueBlot (eBioscience, San Diego, CA) as the secondary antibody. These antibodies were diluted with Can Get Signal immunoreaction enhancer solution (Toyobo, Japan).

Statistical analysis. Student's *t* test was used to determine statistical significance. *P* values of <0.05 were considered statistically significant.

RESULTS

Propagation of Nishigahara, Ni-CE, and CE(NiP) strains in mouse brain. The fixed RV strain Ni-CE causes nonlethal infection in adult mice after i.c. inoculation, whereas the Nishigahara strain and the CE(NiP) strain, which is a chimeric virus with the Nishigahara P gene in the genetic background of the Ni-CE strain, kill adult mice (Fig. 1A) (30). To investigate the mechanisms underlying this difference, we initially examined the propagation of these RV strains in mouse brains. The viral titer of the Nishigahara strain quickly increased and reached 1.3×10^8 FFU/g at 3 days p.i. (Fig. 1C). In contrast, the titer of the Ni-CE strain was less than 10^2 FFU/g at 3 days p.i. and reached a peak of only 1.3×10^4 FFU/g at 6 days p.i. before gradually decreasing during 8 to 10 days p.i. Importantly, strain CE(NiP) grew more efficiently than strain Ni-CE, reaching a titer of 7.9×10^4 FFU/g at 3 days p.i. The different propagation efficiencies of the Ni-CE and CE(NiP) strains at this early stage of infection (3 days p.i.) are consistent with the hypothesis that host innate immunity is involved in the mechanism by which the P gene determines viral pathogenicity.

IFN-α sensitivities of the Nishigahara, Ni-CE, and CE(NiP) strains. Using mouse neuroblastoma NA cells, we previously demonstrated that the attenuated Ni-CE strain is more sensitive to IFN-α than the virulent Nishigahara strain or strain CE(NiP) (30). Next, we confirmed that this is a general phe-

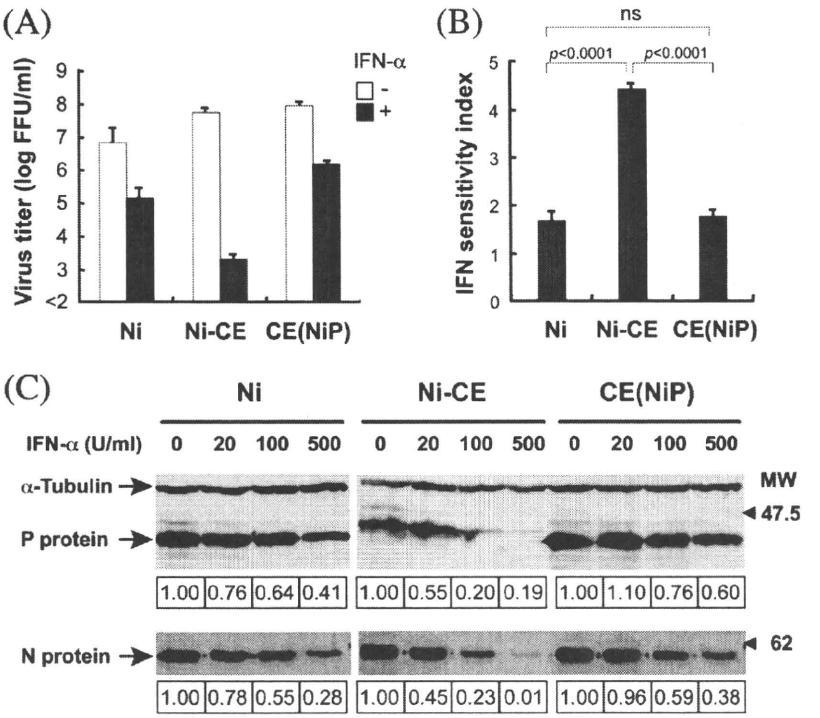

FIG. 2. The Nishigahara (Ni) and CE(NiP) strains are more resistant to IFN-α than the Ni-CE strain in infected human neuroblastoma cells. (A) Growth of each strain in human neuroblastoma SK-N-SH cells in the presence and absence of IFN-α. The cells were inoculated with each virus at an MOI of 0.01 and cultured in growth medium with or without human IFN-α (500 U/ml). The viral titer in the culture medium, collected 3 days p.i., was determined by a focus assay using mouse neuroblastoma NA cells. The data are the means ± standard deviations of three independent replicates. (B) IFN sensitivity index of each strain. The index is the logarithm of the virus titer in SK-N-SH cells (untreated) minus that of the titer in SK-N-SH cells treated with IFN-α (500 U/ml). Each bar represents the mean ± standard deviation of the results of three independent replicates. ns, not significant ($P \geq 0.05$). (C) Viral protein synthesis of each strain growing in SK-N-SH cells treated without or with IFN-α. The cells were inoculated with each virus at an MOI of 0.01 and then were cultured with growth medium containing different concentrations of IFN-α (0, 20, 100, and 500 U/ml). The cell lysate was prepared at 2 days p.i. and analyzed by Western blotting using an anti-P protein rabbit serum or an anti-N protein mouse monoclonal antibody. Alpha-tubulin (α-Tubulin) was used as a loading control. The numbers in the boxes represent relative amounts of RV P or N protein standardized to the amount of the loading control. The amounts of each protein are shown as the ratio, considering the standardized amount in IFN-α-untreated cells (0 U/ml) as 1.00. MW, molecular weight (in thousands).

nomenon in that it can be observed in cell lines derived from different mammalian species. Specifically, we used the human neuroblastoma cell line SK-N-SH and compared the growth of the different RV strains in these cells in the absence or presence of IFN-α (500 U/ml) (Fig. 2A). In the absence of IFN-α, the Nishigahara strain grew less efficiently than the Ni-CE strain, probably due to the fact that strain Nishigahara has been maintained by rabbit brain passages and is not well adapted to the cultured cells. In spite of this, when grown in the presence of IFN-α, the titer of the virulent Nishigahara strain (1.6×10^5 FFU/ml) was significantly higher than that of the avirulent Ni-CE strain (2.1×10^3 FFU/ml). Similarly, the titer of the virulent CE(NiP) strain in the presence of IFN-α (1.5×10^6 FFU/ml) was much higher than that of strain Ni-CE. To standardize the different capacities of these strains for adaptation to the cultured cells, we determined and compared their IFN sensitivity indexes, which represent the log difference between the titers with and without IFN-α treatment (Fig. 2B). The IFN sensitivity index of strain Nishigahara (1.69 ± 0.11 [mean ± standard deviation]) was not different from that of the CE(NiP) strain (1.77 ± 0.10). In contrast, the index of strain Ni-CE (4.43 ± 0.09) was significantly higher than that of strain Nishigahara or strain CE(NiP) ($P <$ 0.0001). This indicates that the Ni-CE strain is approximately 500-fold more sensitive to IFN-α than the Nishigahara and CE(NiP) strains.

Next, we infected SK-N-SH cells with each RV strain and incubated the cells with culture medium containing different concentrations of IFN-α (0, 20, 100, and 500 U/ml). Western blotting revealed dose-dependent decreases in the expression levels of N and P proteins in SK-N-SH cells infected with strains Nishigahara, Ni-CE, and CE(NiP) (Fig. 2C). However, the decrease in the Ni-CE-infected cells was clearly greater than those observed in cells infected with the Nishigahara or CE(NiP) strain. Quantification of the protein band intensities supported this observation (Fig. 2C). These data indicate that in infected human cells, the virulent Nishigahara and CE(NiP) strains are less sensitive to IFN-α treatment than the Ni-CE strain and that the P gene determines the different IFN-α sensitivities of the RV strains.

Nishigahara P protein blocks IFN-α-induced ISRE activity more efficiently than Ni-CE P protein. Vidy et al. (36) and Brzózka et al. (4) previously reported that RV P protein has the capacity to inhibit the IFN signaling pathway. As strains Ni-CE and CE(NiP) are genetically identical except for the P

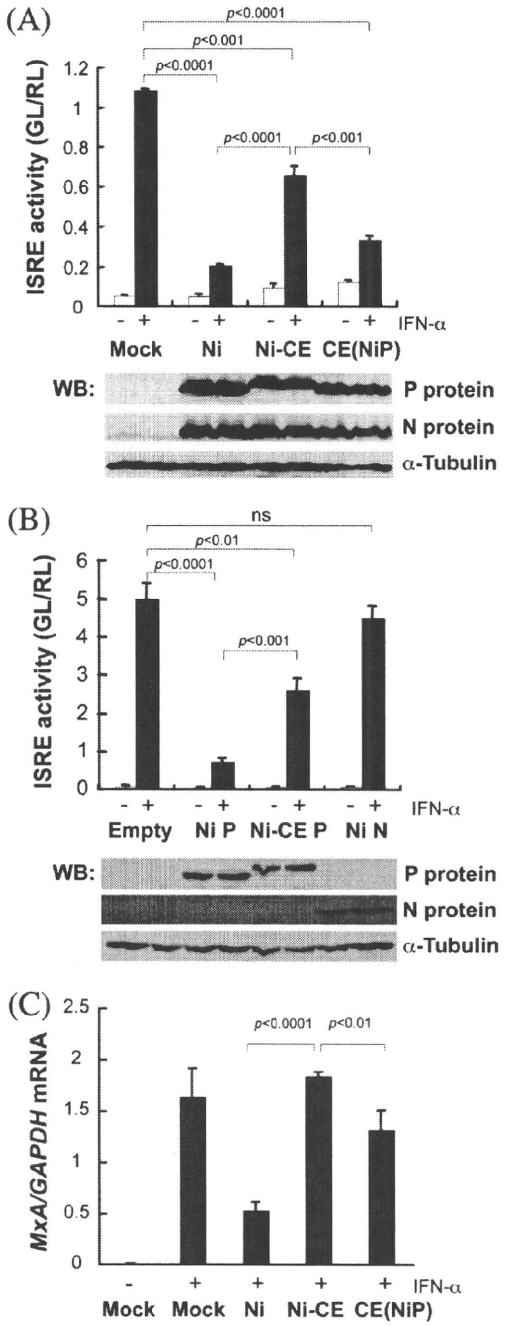

FIG. 3. The extent of inhibition of IFN-α-induced ISRE activity by infection with RV or by the expression of RV P protein differs between RV strains. (A, upper panel) SK-N-SH cells were transfected with the ISRE reporter plasmid (pISRE-Luc) and the control plasmid (pRL-TK) and then inoculated with each virus at an MOI of 3 at 24 h posttransfection. Six hours later, the cells were treated with IFN-α (2,000 U/ml) for 12 h and the cell lysates were subjected to the dual luciferase assay. The data represent firefly luciferase activity (GL) normalized to *Renilla* luciferase activity (RL), presented as the means ± standard deviations of the results of three independent replicates. (B, upper panel) SK-N-SH cells were transfected with the ISRE reporter and the control plasmids together with the expression plasmid encoding Nishigahara or Ni-CE P protein or Nishigahara N protein (pcDNA-Ni P, -CEP, and -Ni N, respectively). At 24 h post-transfection, the cells were treated with IFN-α (2,000 U/ml) for 6 h and the cell lysates were subjected to the dual luciferase assay. GL, firefly luciferase activity; RL, *Renilla* luciferase activity; ns, not significant ($P \geq 0.05$). (A and B, lower panels) Western blot analysis of the cell lysates used for the luciferase assay was carried out using an anti-P protein rabbit serum or an anti-N protein mouse monoclonal antibody. Alpha-tubulin (α-Tubulin) was used as the loading control. (C) Relative expression level of *MxA* mRNA in SK-N-SH cells infected with the Nishigahara, Ni-CE, or CE(NiP) strain. SK-N-SH cells were inoculated with each virus at an MOI of 3 and, 6 h later, were treated with IFN-α (2,000 U/ml) for 12 h. Total RNA was extracted from the cells and subjected to quantitative real-time RT-PCR. The expression levels of the *MxA* gene were normalized to the mRNA levels of *GAPDH*. Each bar represents the mean ± standard deviation of the results of three independent replicates. Ni, Nishigahara; WB, Western blot.

gene but differ in their sensitivity to IFN-α (Fig. 2), we hypothesized that the Nishigahara P protein but not the Ni-CE P protein would be able to efficiently block the IFN signaling pathway. To test this, we examined IFN-induced transcriptional activation in SK-N-SH cells infected with the Nishigahara, Ni-CE, and CE(NiP) strains, using a reporter gene assay with luciferase expression under the control of an ISRE-containing promoter (Fig. 3A). As expected, ISRE-dependent luciferase expression was clearly activated by IFN-α treatment in mock-infected cells, but the luciferase expression was significantly lower in equivalently treated cells infected with the Nishigahara or CE(NiP) strain ($P < 0.0001$) (Fig. 3A, top). Ni-CE infection also inhibited IFN-induced luciferase expression, but the inhibition was significantly weaker than that observed in cells infected with Nishigahara and CE(NiP) strains ($P < 0.0001$ and $P < 0.001$, respectively). Western blotting of cell lysates prepared for the reporter gene assay demonstrated that these strains expressed comparable amounts of P protein (Fig. 3A, bottom). Similar results were obtained with equivalent reporter assays using NA cells infected with each strain (data not shown).

We next examined whether single expression of the Nishigahara or Ni-CE P protein differentially affects IFN-induced luciferase expression by using SK-N-SH cells transfected to express the respective proteins (Fig. 3B). Expression of the Nishigahara or Ni-CE P protein alone significantly decreased IFN-induced luciferase expression compared to the level of expression in the control (empty vector transfected) cells ($P < 0.0001$ and $P < 0.01$, respectively) (Fig. 3B, top). However, the inhibitory effect of Nishigahara P protein was significantly greater than that of Ni-CE P protein ($P < 0.001$), even though the expression level of Ni-CE P protein was comparable to that of Nishigahara P protein (Fig. 3B, bottom). Similar results were obtained in identical assays performed using NA cells (data not shown). In contrast, the expression of Nishigahara N protein alone did not affect ISRE activation in response to IFN-α (Fig. 3B, top), showing that the observed inhibitory effect on IFN signaling is specific to the P protein.

To check whether infections of these RV strains have different effects on the transcription of an endogenous cellular ISG which is controlled by ISRE, we used real-time RT-PCR to compare the expression levels of the *MxA* gene in Nishigahara-, Ni-CE-, and CE(NiP)-infected SK-N-SH cells treated with IFN-α (Fig. 3C). We found that the expression levels of the *MxA* gene in Nishigahara- and CE(NiP)-infected cells were significantly lower than the level in Ni-CE-infected cells ($P <$